Aus der
Medizinischen Klinik und Poliklinik I
Klinik der Ludwig-Maximilians-Universität München
Direktor: Prof. Dr. med. Steffen Massberg

The effect of stromal cell-derived factor 1（SDF1）on the migration of megakaryocyte progenitors: An in vitro analysis

Dissertation
zum Erwerb des Doktorgrades der Medizin
an der Medizinischen Fakultät der
Ludwig-Maximilians-Universität zu München

vorgelegt von
Zheming Liu
aus
Jiangsu, China
2019

Mit Genehmigung der Medizinischen Fakultät

der Universität München

Berichterstatter: Prof.Dr. Steffen Massberg

Mitberichterstatter: Prof.Dr. Andreas Humpe

Mitbetreuung durch den

promovierten Mitarbeiter: Dr. Florian Gärtner

Dekan: Prof.Dr.med.dent. Reinhard Hickel

Tag der mündlichen Prüfung: 21.03.2019

Table of contents

Page number

List of figures

Summary

Our preliminary in vivo experiments showed that megakaryocyte progenitors (MKps) could migrate towards mature megakaryocytes (MKs) under inflammatory stress. It has been reported that MKs can secrete SDF1 (Stromal cell-derived factor1), which is a chemokine protein that stimulates the growth of B cell precursors and is crucial for the maintenance of hematopoietic stem cells (HSCs). SDF1 plays a vital role in the migration of HSCs and HSPCs, however, its role in megakaryopoiesis is still unclear.

Our results showed that MKs can express the SDF1 but in a relatively low level; Instead of mature MKs or TPO triggered MKs, SDF1 can direct the migration of MKps in vitro, which can be inhibited by AMD 3100 (the antagonist of CXCR4). Thirdly, the circulating platelets number in the AMD 3100 treated mice have no statistical significance compared to the control group. Although the number of MKs and MKps in the bone marrow did not change obviously, they were located slightly distant from the vessels in situ in the AMD 3100 treatment group. The AMD3100 cannot significantly prevent platelets recovering in the mice under platelet depletion (PD). In those mice treated with PD and AMD 3100, most of the MKs and MKps in the bone marrow remained close to the vessels and the number of MKs and MKps remained stable.

Taken together, this thesis work endows us with further insight of the physiological property of MKs in vitro and helps us to explore the effect of SDF1

and MKs in the migration of MKps. In the future, this may lead to better understanding of the megakaryopoiesis.

Zusammenfassung

Bisherige Vorarbeiten unserer Arbeitsgruppe beschäftigten sich mit der Rolle von Megakaryozyten und ihren Vorläuferzellen. In vivo konnte von uns gezeigt werden, dass im Rahmen einer Entzündungsreaktion Vorläufer der Megakaryozyten zu reifen Megakaryozyten migrieren. Andere Autoren berichteten, dass Megakaryozyten in der Lage sind SDF-1 (stromal cell-derived factor 1) zu bilden und zu sezernieren. SDF-1 ist ein Chemokin, das das Wachstum von Vorläufer-B-Zellen stimuliert und grundlegend für den Erhalt von hämatopoetischen Stammzellen ist. Es spielt eine essentielle Rolle bei der Migration von hämatopoetischen Stamm- und Vorläuferzellen. Jedoch ist seine Rolle in der Megakaryopoese noch nicht klar.

Unsere Ergebnisse zeigen, dass Megakaryozyten relativ geringe Mengen an SDF-1 bilden. SDF-1 kann Megakaryozytenvorläufer in vitro zur Migration anregen, jedoch nicht reife oder ex vivo durch Thrombopoietin gereifte Megakaryozyten. Diese Migration kann durch AMD 3100, einem CXCR4 Antagonisten, inhibiert werden. Obwohl die mit AMD 3100 behandelten Mäuse, keinen statistisch signifikanten Unterschied in der Thrombozytenzahl im Vergleich zu Kontrolltieren zeigten, hielten sich die Megakaryozyten und ihre Vorläuferzellen im Knochenmark der behandelten Tiere weiter entfernt von Gefäßen auf als in den Kontrolltieren. AMD 3100 zeigte keinen statistisch signifikanten Effekt auf die Regenerierung der Thrombozytenzahlen in Mäusen nach Plättchendepletion. Bei mit PD und AMD 3100 behandelten Tieren konnte

nicht beobachteten werden, dass sich Mks und Mkps weiter vom Gefäß entfernt aufhielten. Mks und Mkps unterschieden sich nicht in ihrer Zellzahl.

Diese Ergebnisse helfen, die physiologischen Eigenschaften von Megakaryozyten besser zu verstehen und beleuchten die Rolle von SDF-1 in Hinblick auf die Migration von Megakaryozyten und ihren Progenitorzellen. Mit Hilfe dieser Resultate soll dazu beigetragen werden, die Megakaryopoese in Zukunft besser zu verstehen.

1. Introduction

1.1 Background

1.1.1 Megakryopoiesis

1.1.1.1 The megakaryopoiesis pathway

Megakaryocytes (MKs) are the biggest cells in the bone marrow, and are in diameter of 50um-100um[1]. Although MKs in the whole bone marrow count is less than 0.01%, one megakaryocyte can grow into 10-20 long cytoplastic protrusions and differentiate into large amounts of platelets in the vessels[2]. The origin of megakaryocyte precursor is hematopoietic stem cell (HSC), which is abundant in fetal liver, yolk sac and bone marrow[3][4][5]. Taken together, there are two pathways that HSCs can differentiate into mature megakaryocytes (Figure 1.1.1.11)[6] .

The classic megakaryopoiesis pathway is from HSCs to megakaryocyte progenitors (MKps) and at last to mature MKs. The steady-state HSCs will give rise firstly to multipotent progenitors (MPPs)[7] and later give rise to common myeloid or lymphoid progenitors (CMPs or CLPs)[8][9]. The CMPs will subsequently differentiate into the granulocyte-macrophage (GMPs) and megakaryocyte-erythroid progenitors (MEPs)[10]. MEPs are the precursors of megakaryocyte progenitors and erythroid progenitors[11]. Some scientists defined a fraction of Lineage-Sca-1+c-kit+ cells (LSKs) as the so-called lymphoid-primed multipotent progenitors (LMPPs)[12]. In these cells the Flt3 is highly expressed in the CD34+ cells and they have the potential to differentiate

into granulocyte, monocyte, B and T cell, however, there is a lack of significant MegE potential. Nevertheless, by using β-actin GFP C57Bl6 Thy1.1 transgenic mice model to test the MegE potential demonstrated that LMPPs retained megakaryocyte potential [13]. Some scientists also shed light on the fact that HSCs are heterogeneous, by using von Willebrand factor (vWF)-eGFP mice, from which they demonstrated that large amounts of HSCs at the apex of hierarchy, are platelet biased[14].

Apart from the classic megakaryopiesis pathway, another situation arises when the hematopoietic system is under stress. To sustain proper blood production and maintain the homeostasis, HSCs and HSPCs can sense hematopoietic stress and react to the inflammatory signals[15][16][17]. Although the lineage commitment and gene expression of HSCs is not clear when the hematopoietic system is under the inflammatory stress, some evidence has presented us with the association between inflammation and megakaryopoiesis[18][19][20][21]. Haas et al. reported that there are some megakaryocyte progenitors sharing some common features with HSCs and can serve as a megakaryocytic pool when exposed to the inflammatory impairment, are defined as the stem cell like megakaryocyte-commited progenitors (SL-MKPs)[6]. These cells can express MK lineage cell marker-CD41, yet the characteristic markers remained unclear. In this experiment they treated the mice with polyinosinic: polycytidylic acid (pI:C) and found that the SL-MKPs can then differentiate into megakaryocytes (Figure 1.1.1.1)[6]. Consequently, the SL-MKPs remain quiescent in the state of

homeostasis and will be activated when they sense hematopoietic stress.

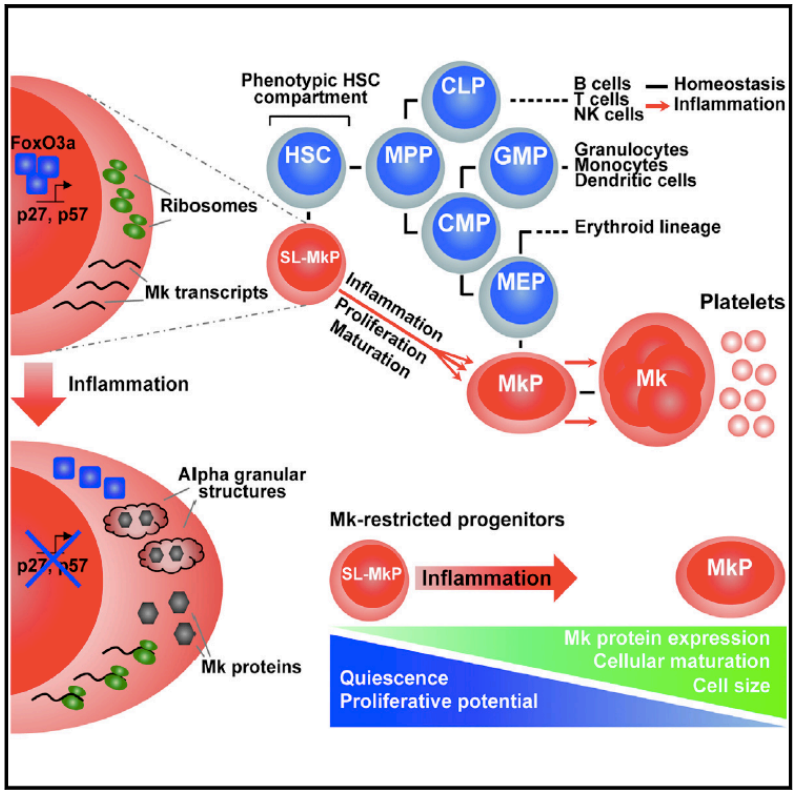

Figure 1.1.1.1 The scheme of inflammatory signaling activated stem-like megakaryocyte progenitors (SL-MkPs)[6].

1.1.1.2 Megakaryocytes polyploidization and differentiation

Giving rise from MKs, approximately $1x10^{11}$ platelets are produced everyday. MKs will differentiate into lots of cytoplasmic protrusions before giving rise to platelets, which are called pro-platelet. MKs are rare cells not only because of their huge volume but also due to their special endomitosis-polyploidy, during which the MK cytoplasm volume will increase in parallel with their ploidy [22][23]. In this way the MKs can increase the capacity of cell cytoplasm potently and then increase the production of platelets. Evidence has proven that the process of MK polyploidization is not obligatory but will benefit the increase in

the generation of platelets[24][25][26]. The DNA content in this process can possess from 2N to 128N. The process of polyploid cells (8N and higher) that give rise to platelets is defined as maturation[23]. Nevertheless, in some pathologic situations the 2N and 4N MKs can also differentiate into platelets[27]. Some scientists also reported these phenomena could be observed in the fetal liver and cord blood[28][29].

There are four stages in the maturation of megakaryocytes. Cells in stage I are the so-called MK progenitors. They are round, with single nucleus and normal membranous organelles, and about 10-15um in diameter[30]. In this stage, the demarcation membrane system (DMS) does not appear in the cells. Few tetraploid MKs arise in this stage[31].

Some characteristic structures start appearing in stage II. The chromosomes are doubled[32]. In this stage we can distinguish the MKs (14-20 um) from their morphology. The nucleus is bigger and some tube-like structures arise, which are considered as the pre-DMS[30]. Considering the cell cycle, the M-phase is obviously decreased. During which the mitotic spindle will be decomposed before the process of chromosomal separation is finished. This will lead to the inability of the chromatids to move to opposite poles of the spindle, and so cell division failed[33]. Megakaryocyte chromosomes will increase 4–8 folds in this stage[30].

With the development of cell maturation, MKs are more distinguishable in stage III. Cell diameter is about 20-40 um. Cell organelles are developed in a large

amount. More higher level MKs (8N, 16N, 32N) arise in this stage and the smaller nucleoli indicated that the transcription and protein synthesis has stopped[30]. The megakaryocytes will develop into even bigger cells (40-60 um) in stage IV. The characteristic structure is the pro-platelet formation and disappearance of nucleolus[34]. DMS spread and divide the cytoplasm evenly into proplatelets. The proplatelets will penetrate into vessels and platelets will separate from each other in the blood[35]. Figure 1.1.1.2.1[30] is the representative picture of the whole four stages of megakaryocyte differentiation.

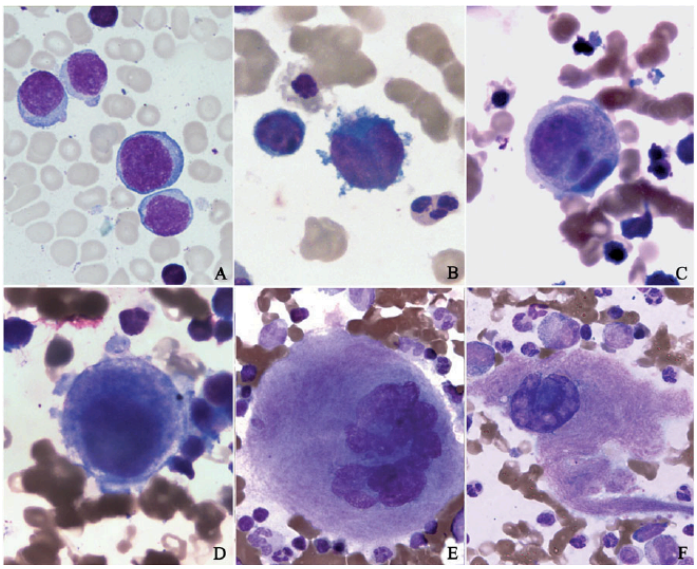

Figure 1.1.1.2.1 Morphologic development of megakaryocytes[30]. (A) Stage I cells. (B) Stage II cells. (C, D) Stage III cells with a diameter of 20–40 mm. (E) A stage IV cell. (F) A mature megakaryocyte is releasing platelets.

Different cell surface markers can help us to distinguish the megakaryocyte lineage cells. CD41 is the widely accepted marker that expressed on the whole stages of megakaryocyte[36]. Some other studies also revealed that C-kit，vWF (von Willebrand factor) and CD150 are the surface markers in the whole stages of megakaryopoiesis [6][14][37][38]. CD42, PF4 and GPVI act as late stage

markers [36][39][40][41] (Figure 1.1.1.2.2)[Dissertation, Wenwen Fu, LMU, 2017].

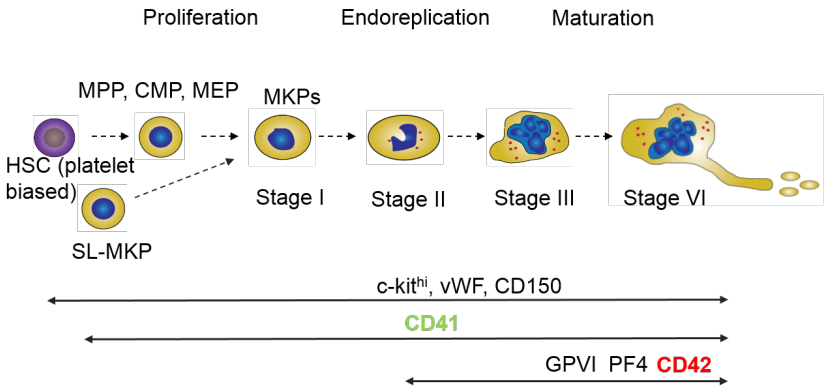

Figure 1.1.1.2.2 Megakaryocyte differentiation scheme and expression of related markers at different cell stages[Figure and legend, Dissertation Wenwen Fu, LMU, 2017]

1.1.1.3 Transcriptional regulation of megakaryopoiesis

MEPs are bipotential precursors that can differentiate into cells of either erythroid or megakaryocytic lineages[8][42]. Abundant transcription factors such as Runx1, Gata1, Fli1, c-Myb, interleukin-9 and PLZF/miR-146a/CXCR4 will accelerate or suppress the differentiation of MKs.

GATA-1 is a transcriptional factor (TF) that plays crucial role in megakaryopoiesis. The knockout or knockdown mice of GATA-1 can develop megakaryocytes, but MKs will have reduced polyploidy and cannot produce platelets both in vivo and in vitro[43][44]. In GATA-1^{low} mice the MEPs can give rise not only to erythroid cells and megakaryocytes, but also to mast cells[45]. FOG-1 can cooperate with GATA-1 and contributes to megakaryopoiesis in the early stage. In the FOG-1 knockout mice no MKs linage cells can be produced [46].

RUNX1 is essential in the regulation of megakaryopoiesis and thrombopoiesis. In particular, the knockout of RUNX1 mice presented an obvious decrease in polyploidization and platelet level[47]. RUNX1 has 2 promoters: the distal P1 and proximal P2 promoters. Julia Draper et al. found that the P1 knock-in MEPs in the P1-MRIPV (Runx1 P1 knock-in of RUNX1B) mice are erythroid cell biased. They also found that RUNX1B can modulate endomitosis and thrombopoiesis [48]. Olga Kuvardina et al. reported that RUNX1 inhibits the differentiation of MEPs and CD34+ progenitor cells into erythroid cells[49]. Which is achieved through the genetic inhibition of erythroid regulator KLF1.

Some transcriptional factors like GFI-1B, NF-E2 and c-myb contribute to both megakaryopoiesis and erythropoiesis. GFI-1B plays crucial role in the late maturation of MKs and MKps in the GFI-1B deficient fetal liver can only differentiate into small megakaryocyte colonies. The cells expressed low levels of MK common markers like von-Willebrand factor, c-mpl and GPIIb[50]. NF-E2 is essential for the expression of megakaryocyte genes and the NF-E2 knock-out mice present severe thrombocytopenia[51][52]. c-myb can direct the differentiation of megakaryocytes and macrophages[53], and its defect will lead to excess megakaryopoiesis and followed by increased platelet biosynthesis [54].

GABPa, ETS1 and Fli-1 are ETS (E26 transformation-specific) proteins, which are expressed in megakaryocytes and play vital roles in cell development. Fli-1 is crucial in the development of MKs and its defect will lead to thrombocytopenia[42][55]. GABPa is an early stage megakaryocyte gene

regulator, which is essential in the development of fetal liver MKs and expression of cell markers like c-Mpl[56]. ETS1 increases during the maturation of megakaryocyte and decreases in the development of erythroid cells. The overexpression of ETS1 will present a megakaryocyte bias[57].

The microRNAs modulation is crucial in megakaryopoiesis. The miR-150 can decrease c-Myb expression, which may decide the differentiation fate of MEPs [58]. The promyelocytic leukaemia zinc-finger (PLZF) will affect the expression of miR-146 and CXCR4 and indirectly affect the proliferation, differentiation and maturation of MKs and MKps[59]. The inhibition of miR-146 will increase CXCR4 expression, and thus accelerate the maturation and proliferation of MKs. The knockdown of PLZF or CXCR4 will lead to the impairment of megakaryopoiesis.

Thrombopoietin (TPO) and its receptor-MPL, are the most important factors in megakaryopoiesis [60]. The MPL promoter regulates specific expression on the cell surface of megakaryocyte lineage cells, which is a homodimeric type I trans-membrane protein that in relation to the tyrosine kinase Janus kinase 2 (JAK2) signaling. However, TPO is not indispensable for megakaryocyte maturation and platelet biosynthesis[61][62].

1.1.2 Thrombopoiesis

Thrombopoiesis is the whole process in which platelets are assembled and released (Figure 1.1.2.1)[1]. Mature MKs extend long cytoplasm protrusions into bone marrow sinusoidal vessels[63]. The pseudopodium-like protrusions are the origin of platelets, which are called proplatelets. Proplatelets are composed of

swellings, schaft, branch point and tips (Figure 1.1.2.2)[63][64]. Proplatelet budding from mature MKs and can be observed both in vivo [65][66] and in vitro[34][64][67][68][69]. Although large amounts of researches about the production of proplatelet have been conducted, the definite mechanisms of the formation of proplatelet remain unclear.

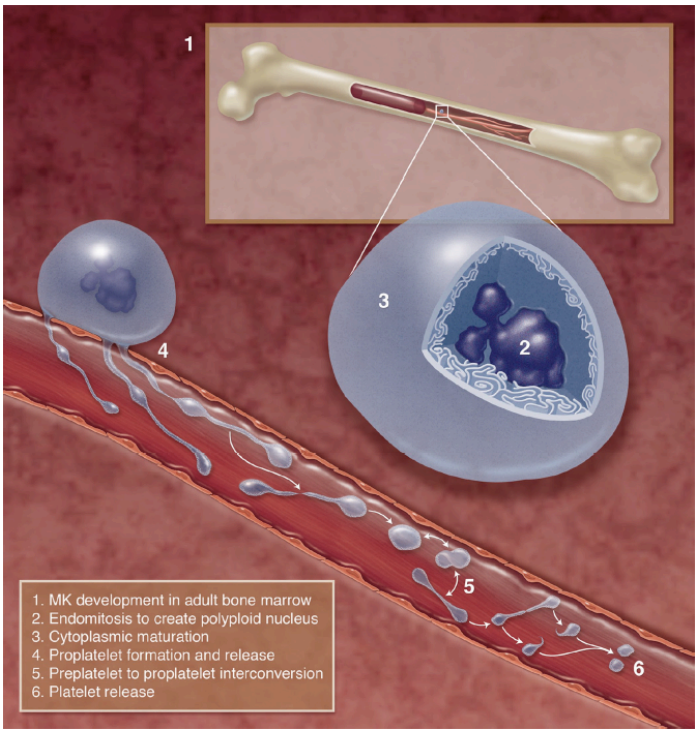

Figure 1.1.2.1 Schematic of platelet production[1].

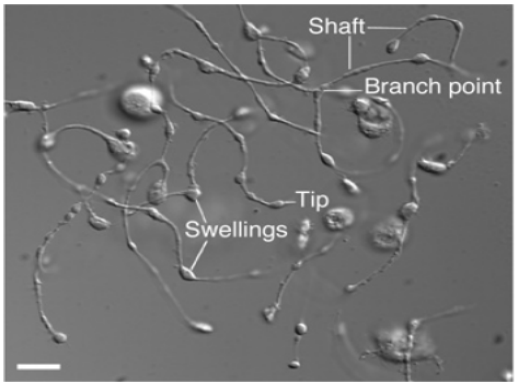

Figure 1.1.2.2 Anatomy of a proplatelet[64].

The cytoskeleton system is essential to the production and function of proplatelet. It has been reported that β 1-Tubulin is the main tubulin isoform in MKs and it plays a vital role in proplatelet formation and elongation[70][71]. Lack of this will lead to thrombocytopenia in both human and mice[72][73]. Through the microtubules it is much more convenient for the transportation of organelles and granules from MKs to proplatelets[2].

The production of proplatelet is the result of complex interaction of mature MKs with bone marrow niches[1]. The vascular niche contains large amounts of different kinds of cytokines and extracellular matrix proteins[74][75][76]. The CXCL12-CXCR4 axis can attract MKs to migrate towards the vessels[77][78]. Fibrinogen and fibronectin are important factors to trigger the sprouting of proplatelet from MKs[79]. Besides the vascular niche, the osteoblastic niche can also help to modulate this process. Some scientists have observed that the osteoblastic niche can provide abundant collagen I, which benefits the MKs proliferation and maturation, yet inhibits proplatelet formation[80][81][82].

It is well known that proplatelet develops from mature MKs and penetrates into vessels to differentiate into platelets[63]. But how the podosome-like structures find their way into vessels remains to be addressed. Schachtner et al. found that MKs can sense the cavity of vessels and then the protrusions will degrade the extracellular matrix proteins, which help proplatelets to extend into vessels [83]. And before proplatelets are released from MKs, the shaft can bend and sprout a

new tip as shown in Figure 1.1.2.3[64]. In this way each megakaryocyte can produce more platelets[64].

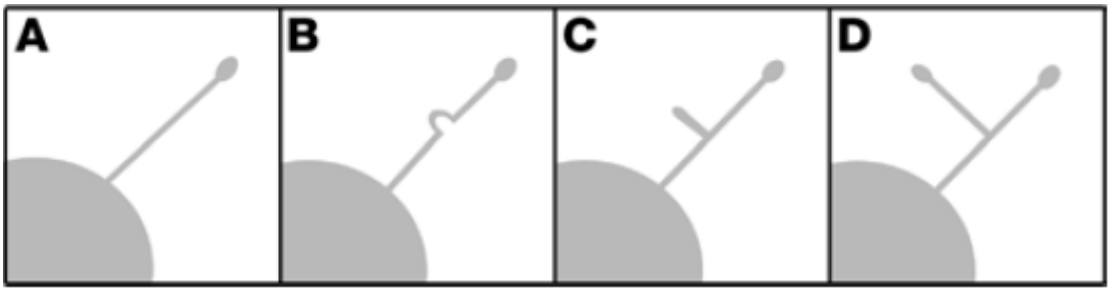

Figure 1.1.2.3 Proplatelet amplification[64].

After the cytoplasm extending into the vessels, some factors will decide platelets release. Junt et.al found that more proplatelets were produced when MKs were activated [65]. Lin Zhang et.al found that the S1p-S1pr1 axis was essential to the extension and release of proplatelets[66]. They observed that the S1p gradient could induce proplatelets extending into vessels in vivo through the 2-photon microscopy. The S1p receptor1 deficient mice will exhibit serious thrombocytopenia. And MKs can produce more proplatelets when S1p-S1pr1 is triggered.

Meanwhile, some scientists have also reported that there do exist the so-called preplatelet[67][84]. As it is showed in Figure 1.1.2.1(number 5)[1], platelets can transform into the structure composed of two independent platelets.

1.1.3 Preliminary in vivo studies of MKs and MKps in the bone marrow

Due to the limitation of imaging techniques, the spatial distribution of MKs remained illusive for a long time. Only recently, with the use of 2-photon intravital microscopy, have scientists got the chance to deeply explore the bone

marrow spatial structure and clearly present the position of mature megakaryocytes[85]. Our preliminary experiments showed that most of the MKs locate close to sinusoids vessels. The bone marrow whole-mount staining data also showed that more than 80% mature MKs attached to sinusoids vessels (Figure 1.1.3.1 and Figure 1.1.3.3 A) and nearly 70% MKps stayed close to the vessels (Figure 1.1.3.2 and 1.1.3.3 B) [Dissertation, Wenwen Fu, LMU, 2017].

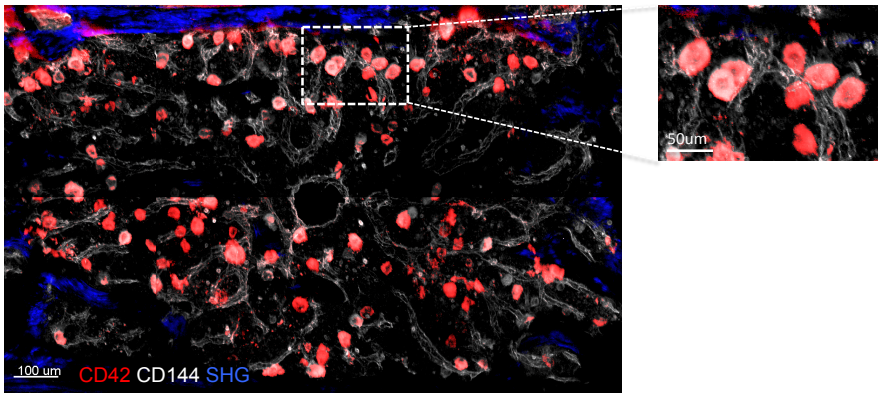

Figure 1.1.3.1 Representative whole-mount immunostaining of mature megakaryocytes in murine sternum bone. CD42 labeled mature MKs. CD144 labeled endothelial cells. The blue signal indicates the bone structure from the SHG. Scale bar= 100µm. [Figure and legend, Dissertation Wenwen Fu, LMU, 2017]

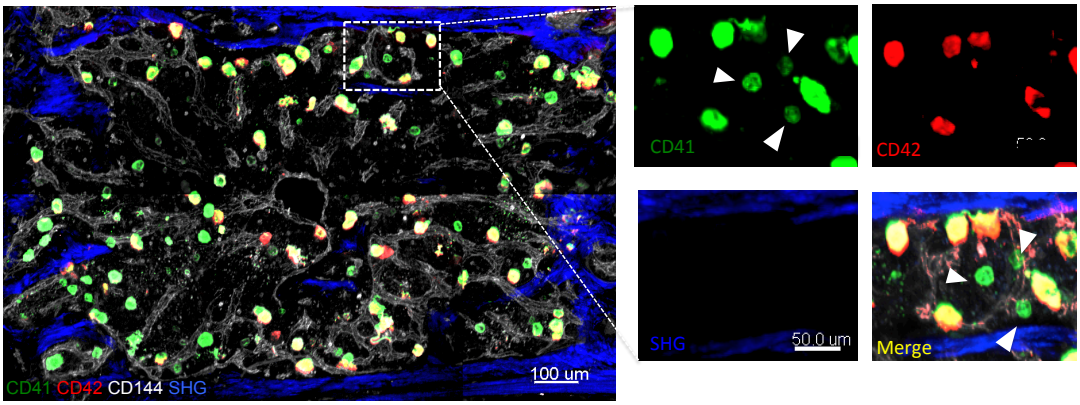

Figure 1.1.3.2 Representative whole-mount immunostaining of megakaryocyte progenitors and mature megakaryocytes in murine sternum bone. CD41 labeled early and late stage of MKs. CD42

labeled mature MKs. CD144 labeled endothelial cells. The blue signal indicated the bone structure from the SHG. Arrowhead indicated MK progenitors. Scale bar= 100μm. [Figure and legend, Dissertation Wenwen Fu, LMU, 2017]

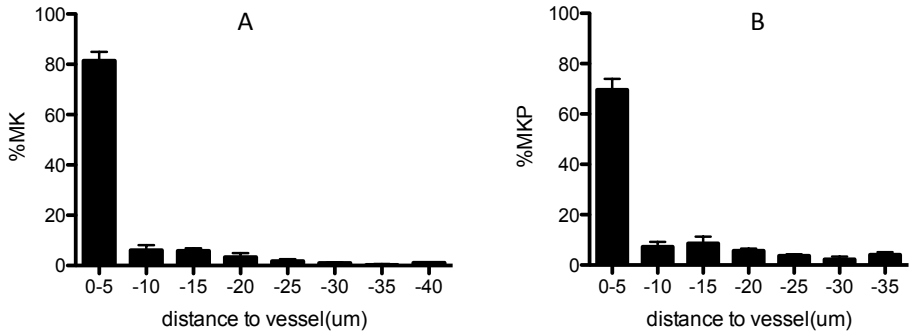

Figure 1.1.3.3 Distance from MKs and MKps to vessels, and the percentages of MKs and MKps. (A) The distance between MKs and vessels. (B) The distance between MKps and vessels. [Figure and legend, Dissertation Wenwen Fu, LMU, 2017]

To investigate the megakaryopoiesis in the bone marrow under stress, they treated the mice with platelet depletion antibody and found that most of the mature MKs stayed stably close to the vessels (Figure 1.1.3.4)[Dissertation, Wenwen Fu, LMU, 2017]. Large amounts of MKs differentiate into platelets after platelet depletion. What was interesting is that the number of MKs remains stable (Figure 1.1.3.6)[Dissertation, Wenwen Fu, LMU, 2017], which indicates that the bone marrow niche is able to replenish the loss of MKs and balance the MK homeostasis.

However, more MKps appeared close to the vessels within a short time (Figure 1.1.3.5 and Figure 1.1.3.7) [Dissertation, Wenwen Fu, LMU, 2017]. A lot of MKps stayed close to the vessels and some of them attached to mature MKs.

Next they treated the vWF-eGFP mice with platelet depletion antibody and after

12h the live imaging was performed with the two-photon microscopy. From the time-lapse video they found that a megakaryocyte progenitor (with white arrow) moved towards the megakaryocyte (the stable big green cell)(Figure 1.1.3.8) [Dissertation, Wenwen Fu, LMU, 2017]. The number of MKps that attached to MKs was then calculated and they found that compared with the control group, there are obviously more MKps attached to MKs (Figure 1.1.3.9)[Dissertation, Wenwen Fu, LMU, 2017]. The result has statistical significance.

TPO is the most important cytokine in megakryopoesis[60]. Thus besides the platelet depletion stimuli, they also investigated the megakaryopoiesis in the bone marrow that triggered by TPO. They concluded that TPO treatment increases the number of MKps and MKs. However, the increase of MKps number has no statistical significance compared to the platelet depletion group (Figure 1.1.3.10 and Figure 1.1.3.11)[Dissertation, Wenwen Fu, LMU, 2017]. In spite of that the fraction of MKps that attached to MKs in TPO treatment group was significantly increased (Figure 1.1.3.11 C)[Dissertation, Wenwen Fu, LMU, 2017]. As MKps proliferated potently and reached a peak level within 24h after platelet depletion (Figure 1.1.3.6) [Dissertation, Wenwen Fu, LMU, 2017], they then measured the level of TPO in the serum through Elisa. The result showed that the TPO level reached a peak within 12h after platelet depletion (Figure 1.1.3.12) [Dissertation, Wenwen Fu, LMU, 2017]. This also means that the signal to accelerate megakaryopoiesis driven by platelet depletion is strongest at the time point of 12h after the stimulation. They next conducted EdU (5-ethynyl-2'

-deoxyuridine) experiment through flow cytometry to test the proliferation of MKps after 12h of platelet depletion. As it is showed in Figure 1.1.3.13, there is a substantial increase in the fraction of proliferating MKps [Dissertation, Wenwen Fu, LMU, 2017].

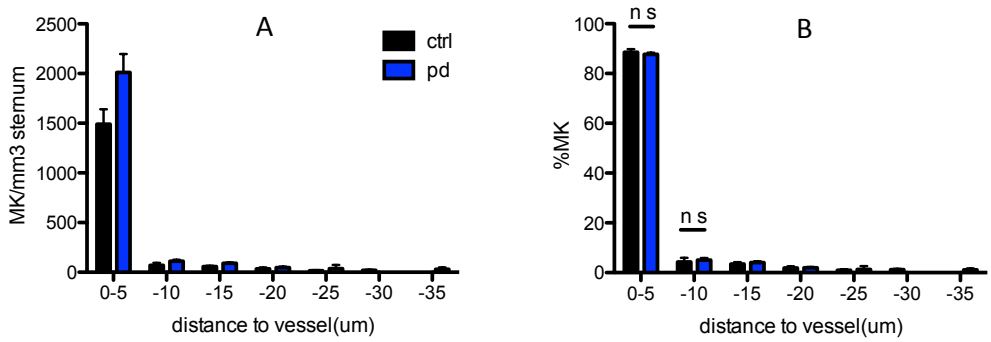

Figure 1.1.3.4 Distance between MKs and the vessels. (A) the number of MKs per 1mm3 sternum bone marrow in platelet depleted 12h mice (blue) and control mice (black). (B) the percentage of MKs in platelet depleted 12h mice (blue) and control mice (black). The distances are binned into 5-μm intervals. n=4 in each group. Error bar=SEM. [Figure and legend, Dissertation Wenwen Fu, LMU, 2017]

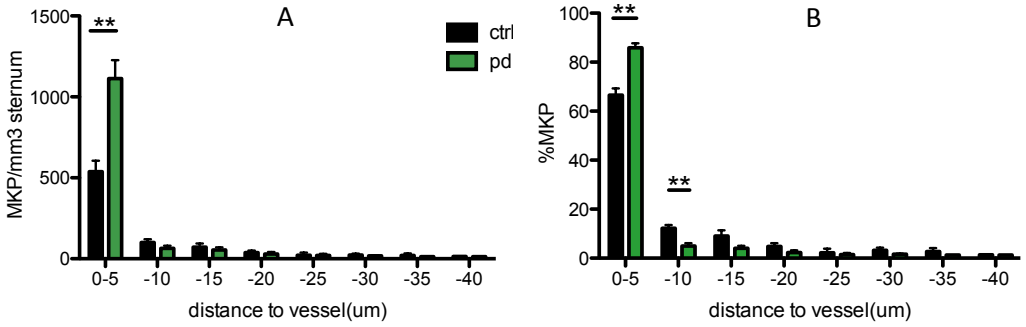

Figure 1.1.3.5 Distance between MKps and the vessels. (A) the number of MKps per 1mm3 sternum bone marrow in platelet depleted 12h mice (green) and control mice (black). (B) the percentage of MKPs in platelet depleted 12h mice (green) and control mice (black). The distances

are binned into 5-µm intervals. n=4 mice per group. Unpaired t-test; P=0.0049; error bar=SEM.

[Figure and legend, Dissertation Wenwen Fu, LMU, 2017]

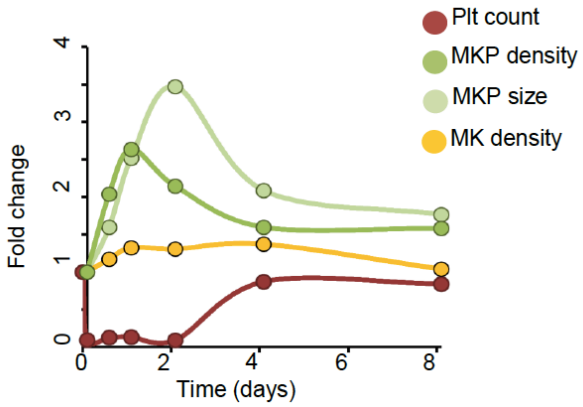

Figure 1.1.3.6 Fold change of platelet count, MKP density (number/mm3 marrow), MKP size and MK density after platelet depletion. Platelet count was gained from peripheral blood measurement. MKs and MKPs was quantified in whole-mount sternum staining from ≥3 mice in each group. [Figure and legend, Dissertation Wenwen Fu, LMU, 2017]

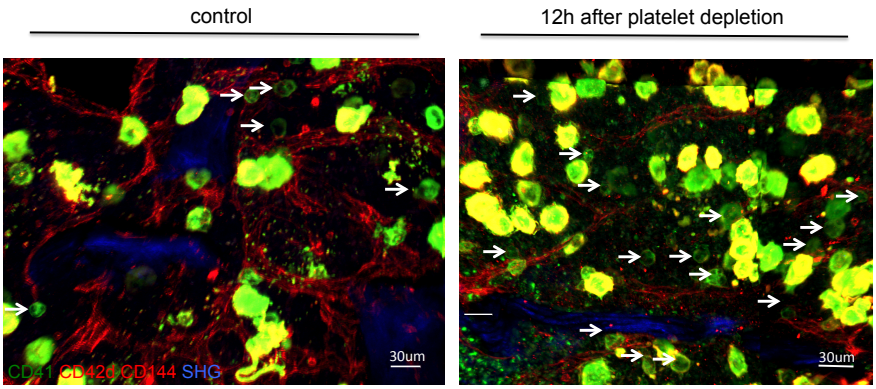

Figure 1.1.3.7 The whole-mount staining of the sternum bone marrow. There are more MKs (CD41+CD42+) and MKps (CD41+CD42-, with white arrow) in the bone marrow 12h after platelet depletion. Scale bar = 30 µm. [Figure and legend, Dissertation Wenwen Fu, LMU, 2017]

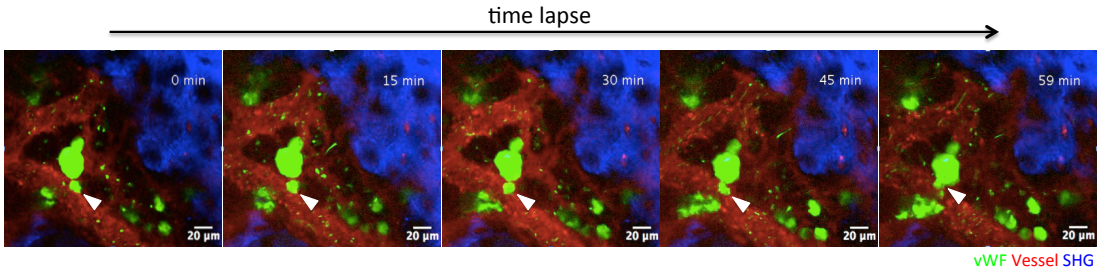

Figure 1.1.3.8 Snaptshots from a calvarial live imaging movie from a vWF-eGFP mouse. Dextran -TRITC was injected intravenously for the vascular label. SHG shows the bone structure. Arrow indicates a MK. Arrowhead indicates a migrating MKP. Scale bar= 20µm. [Figure and legend, Dissertation Wenwen Fu, LMU, 2017]

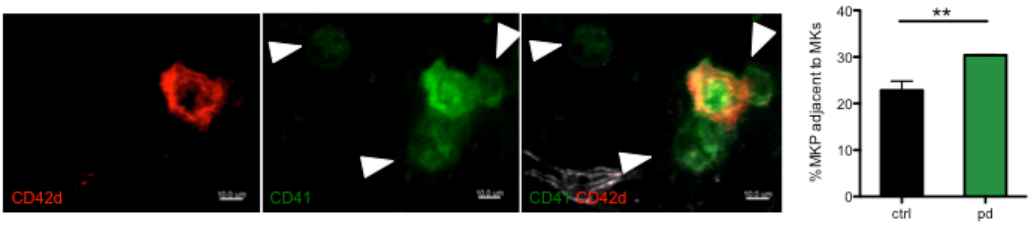

Figure 1.1.3.9 Representative whole-mount immunostaining of megakaryocytes and progenitors in murine sternum. CD42 labeled mature MKs. CD41 labeled early and late stage of MKs. Arrowheads indicate MKPs. Scale bar= 10µm. The histogram present the fraction of MKps that attached to the MKs in the wild type mice and mice after the platelet depletion. ** means p<0.001. unpaired t-test is used. Error bar=SEM. [Figure and legend, Dissertation Wenwen Fu, LMU, 2017]

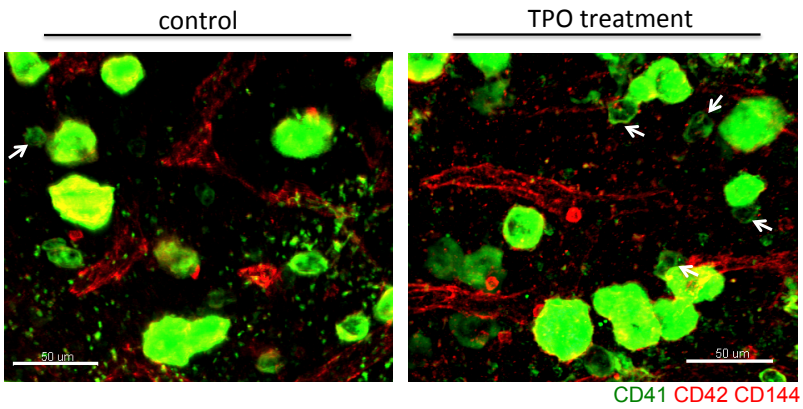

Figure 1.1.3.10 Representative whole-mount immunostaining of MKs, MKPs and vessels in sternum bone marrow of WT mouse and mouse treated with TPO. CD41 (green) labeled early and late stage of MKs. CD42 (red) labeled mature MKs. CD144 (red) labeled endothelial cells. Arrows indicate MKPs which directly attach to MKs. Scale bar =50μm. [Figure and legend, Dissertation Wenwen Fu, LMU, 2017]

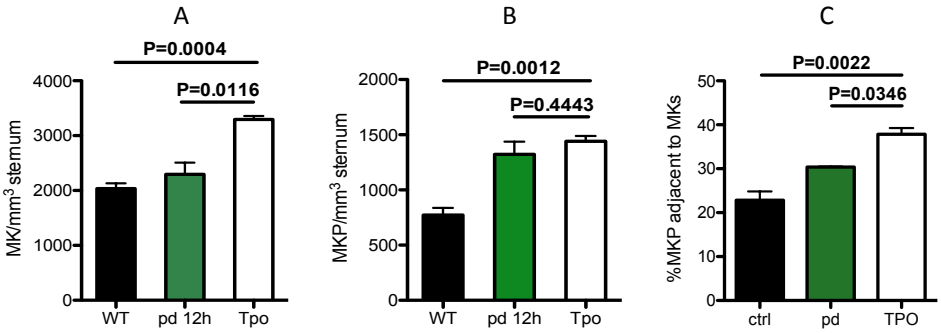

Figure 1.1.3.11 The number of MKs, MKps and fraction of MKps that attached to MKs in WT mice, 12h after platelet depletion, and mice received 3 days TPO injection. (A) Number of MKs per mm3 sternum marrow in WT mice, 12h after platelet depletion, and mice received 3 days Tpo injection. (B) Number of MKPs per mm3 sternum marrow in WT mice, 12h after platelet depletion, and mice received 3 days Tpo injection. (C) Percentage of MKPs that are in direct contact with MKs in control mice that received platelet isotype control antibody injection, 12h after platelet depletion, and mice received 3 days Tpo injection. [Figure and legend, Dissertation Wenwen Fu, LMU, 2017]

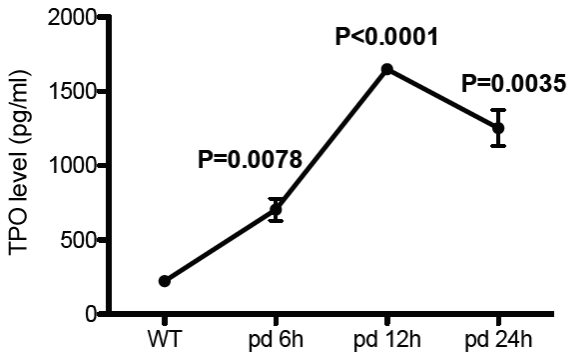

Figure 1.1.3.12 In situ TPO level. Serum is isolated from wild type mice and mice treated with platelet depletion at different time points. [Figure and legend, Dissertation Wenwen Fu, LMU, 2017]

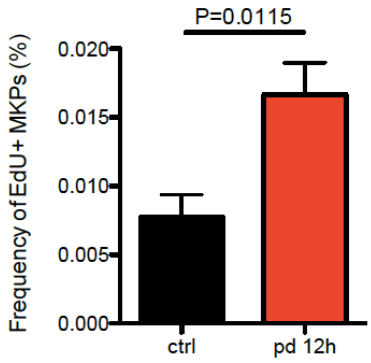

Figure 1.1.3.13 Frequency of EdU+ MKPs in the bone marrow of mice at the time point of 12h after injection of anti-CD42 antibody and isotype control antibody. [Figure and legend, Dissertation Wenwen Fu, LMU, 2017]

1.1.4 SDF1/CXCL12

SDF1 (or CXCL12) is short for stromal cell derived factor1 (formally known as pre B cell derived fator1). In humans it is a chemokine protein encoded by the CXCL12 gene on chromosome 10[86]. Chemokines are 8-12 kDa small molecules and through binding to their receptors on the surface of cells they are able to trigger chemotaxis of cells to concentration gradient[87]. On account of the

difference in N-terminal of cysteine, chemokines are classified into four main subfamilies that are C-, CXC-, CC-, and CX3C[88]. CXCl12 is a highly conserved protein with around 92 amino acid (aa), which have in all six isoforms: α, β, γ, δ, ε, and φ[89][90].

The receptor of CXCL12 is CXCR4 (also known as LESTR, Fusin, and CD184), first discovered on circular leukocytes[91], one of the G protein coupled receptors (including Gα, Gβ, and Gγ subunit.). Among the sub-group members of Gα, the CXCL12/CXCR4 axis is functioned primarily by activating heterotrimeric Gαi-proteins[92][93][94].

CXCL12 is largely expressed in several organs such as lungs, heart, liver, kidney, brain, skeletal muscle and bone marrow[95]. It is an important factor in the migration, differentiation and gene transcription in different cancer cells[92].

Like CXCL12, CXCR4 also broadly expressed on many different cell types, for example, lymphocytes, hematopoietic stem cells, endothelial and different cancer cells[92][96][97]. According to multiple reports, CXCR4 is crucial in the chemo-attract effect in leukocyte and that's maybe why it is a "star" factor in many autoimmune diseases[98][99].

A bulk of studies about CXCL12-CXCR4 axis are focused on its function in the homeostasis of niche systems (including HSCs niche, vascular niche, bone marrow niche and so on), cardiovascular diseases and neurogenesis [100][101][102][103].

Besides binding to CXCR4, CXCL12 can alternatively bind to anther chemokine receptor, CXCR7 (or RDC1), which compared with CXCR4 can be even more affinitive combined to CXCL12(Figure 1.1.4.1)[104][105][106]. The CXCR7 depletion mice will be perinatally lethal and correlated with some cardiovascular diseases[107][108].

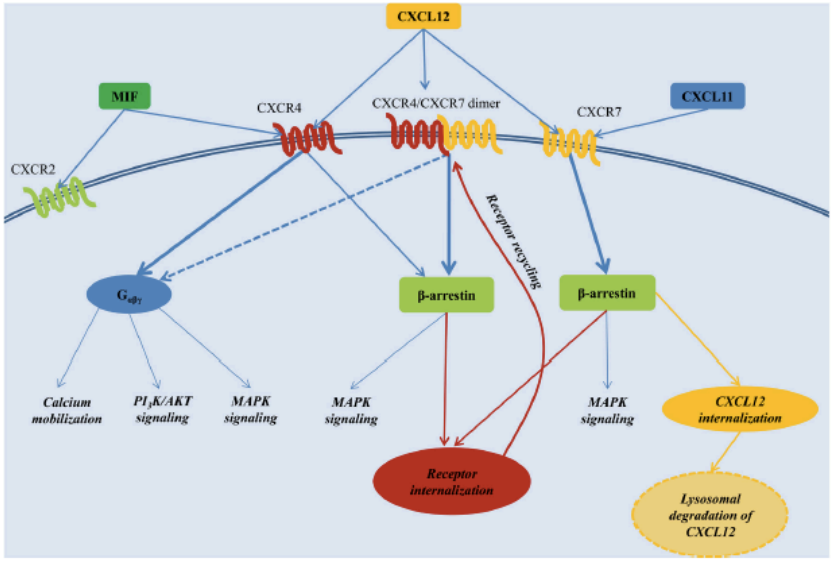

Figure 1.1.4.1 The CXCL12 signaling network[106].

CXCL12 is mainly secreted by osteoblasts, mesenchymal stromal cells, and endothelial cells in the sinusoids of bone marrow[109][110][111][112][113][114]. CXCL12/CXCR4 axis is essential in hematopoiesis, including hematopoietic progenitors homing, retention and proliferation, maintenance of stem cells, proliferation and maintenance of B and common lymphoid progenitors[100][103][110][115]. The mice that are deficient of CXCL12 or CXCR4 die perinatally due to defect of ontogeny[100][101][102][103]. Selectively deleted CXCL12 from osteoblasts could not obviously affect HSCs. However, when CXCL12 is deleted from stromal cells, endothelial cells and nestin-negative mesenchymal

progenitors will seriously affect the homeostasis of HSCs in different degrees [113].

Except these effects, some scientists also found that the CXCL12/CXCR4 axis is crucial to megakaryopoiesis and thrombopoiesis[77][116][117][118]. They reported that SDF-1 accelerates megakaryopoiesis and benefits both MKs and MKps to migrate to the vascular niche. Of greater interest is the report by Lisa et al. that SDF1 relocates megakaryocyte after irradiation[118]. Furthermore, the change of SDF1 level in bone marrow can temporally modulate the location of MKs. The change of MKs location will subsequently lead to the fluctuation of peripheral blood platelets.

An in vitro trans-migration experiment testified that MKs can definitely express CXCR4 and can migrate towards the SDF1 gradient through the bone marrow endothelial cell (BMEC) layers[116]. Considering this effect, William J et al. reported that MMP9, which is induced by SDF1 triggered MKs, can help the SDF1-MKs trans-migration[117]. Scott T Avecilla et al. reported that SDF1 cooperated with fibroblast factor 4 (FGF4) to modulate thrombopoiesis[77]. In their experiment, they found that without the existence of TPO or bone marrow endothelial cells, neither FGF-4 nor SDF-1 is able to improve the proliferation of megakaryocyte progenitors alone. This suggests that the two cytokines can affect the differentiation and proliferation of MKs through affecting their contact to the endothelial cells in the bone marrow. Their results also support the findings of

Hodohara, K. et al.[119] that SDF1 will only promote the maturation of MKps in the presence of TPO.

In conclusion, despite ever more studies focusing on megakaryopoiesis, many questions still remained to be addressed. Whether it is the mature megakaryocytes which attract the MKps to migrate towards them or not? If so, which kind of chemokine do they secrete? In particular, will this be SDF1? Whether MKs can attract the migration of MKps through SDF1 secretion or not, we then investigate the roles of MKs and SDF1 in the migration of MKps.

1.2 Objective

(1). The expression of SDF1 in the bone marrow derived megakaryocytes

The first aim of this thesis is to establish the bone marrow derived megakaryocytes in vitro culture model. We then test the purity and maturity of the megakaryocytes, and to further test whether the megakaryocytes can express SDF1.

(2). The function of SDF1 in the migration of megakaryocyte progenitors (MKps) towards mature megakaryocytes (MKs)

Our preliminary in vivo experiment showed that MKPs can migrate towards mature MKs. Our aim is to isolate the MKPs and to testify the MKs-MKps migration in vitro. After that we further explore the mechanism based on our observations. Hence, the transwell experiment will be a good model to test whether MKps can migrate towards MKs and it also helps us to test the candidate chemokines or cytokines. As our in vivo experiment found that TPO can trigger MKps attachment to MKs, we also use the TPO and TPO treated MKs to conduct the trans-migration experiment.

Later we block the CXCR4 to investigate which role that SDF1 plays in the MK-MKps migration. At the same time, the expression of CXCR4 on the surface of MKps is tested through the flow cytometry.

2. Materials and methods

2.1 Material

CD41 antibody was purchased from Invitrogen eBioscience (Thermo Fisher Scientific, MA, USA). SDF1 mouse anti-mouse/human antibody was purchased from R&D Systems (Minneapolis，USA) and prepared according to the manuals. Pacific Blue anti-mouse TER-119/Erythroid Cells Antibody, anti-mouse Ly-6G/Ly-6C (Gr-1) Antibody, anti-mouse/human CD11b Antibody, anti-mouse CD3 Antibody and anti-mouse CD8a Antibody; PE/Cy7 anti-mouse Ly-6A/E (Sca-1) Antibody; APC anti-mouse CD117 (c-Kit) Antibody; PE anti-mouse Ly6G Antibody and CD42d hamster anti-mouse antibody were purchased from Biolegend (San Diego, CA, USA). CD41-FITC antibody was purchased from Thermo Fisher Scientific Company (San Diego, USA). Mouse anti mouse SDF1 antibody was purchased from R&D Systems (Minneapolis, USA). SDF1 (D32F9) Rabbit mAb was purchased from Cell Signaling Technology (MA, USA). Lineage depletion Kit was purchased from Miltenyi Biotec and used according to the manuals. Transwell inserts were purchased from Corning (New York, US). Plerixafor (AMD3100) was purchased from MedChem Express (New Jersey, USA).

2.2 Mice model

2.2.1 vWF-eGFP mouse model

vWF (known as von Willebrand Factor) is, a multimeric glycoprotein, widely expressed in the endothelial cells and megakaryocyte lineage cells[14][120]

[121], which plays a crucial role in platelet aggregation. In this mouse strain, GFP labels endothelial cells and MK lineage cells including platelet-biased stem cells, MKps, MKs as well as platelets (Figure 2.2.1.1[14] and Figure 2.2.1.2[Dissertation, Wenwen Fu, LMU, 2017]). However, in our preliminary in vivo experiment we were unable to observe any GFP+ endothelial cells under the 2-photon microscopy, which may due to the heterogeneity of vWF in different tissues and cells. And we proved that the vWF is a specific MK lineage cell marker (Figure 2.2.1.2 and Figure 2.2.1.3) [Dissertation, Wenwen Fu, LMU, 2017] and that the numbers and size of MK lineage cells show no obvious differences compared with wild-type mice (Figure 2.2.1.4) [Dissertation, Wenwen Fu, LMU, 2017]. This indicates that the vWF-eGFP mouse strain is a suitable model for megakaryopoiesis research.

Cell types	vWF-eGFP
LSK CD150+CD48-CD34-	60%
MKP(LSK CD150+CD41+)	68%
preMegE	6.56%
platelet	99.8%
bone marrow endothelial	52%

Figure 2.2.1.1 The fraction of different vWF-eGFP+ cells [14].

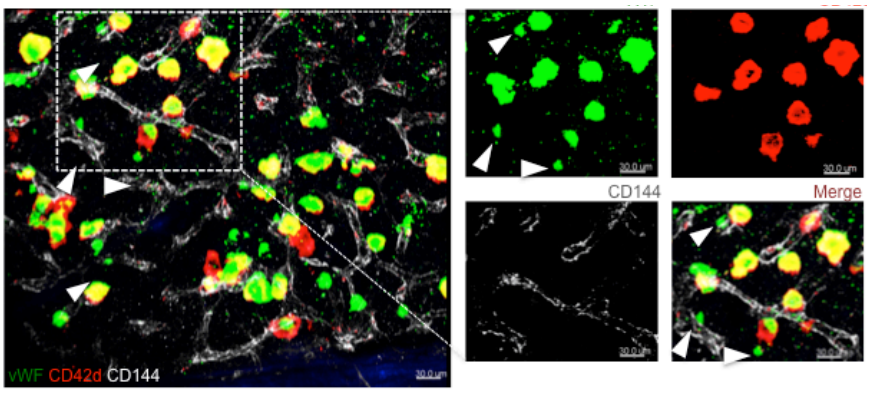

Figure 2.2.1.2 Representative whole-mount immunostaining of megakaryocytes in femur of vWF-eGFP mouse. CD42 labels mature MKs. CD144 labels the endothelial cells. Arrowhead indicated MK progenitors. Scale bar=30μm. [Figure and legend, Dissertation Wenwen Fu, LMU, 2017]

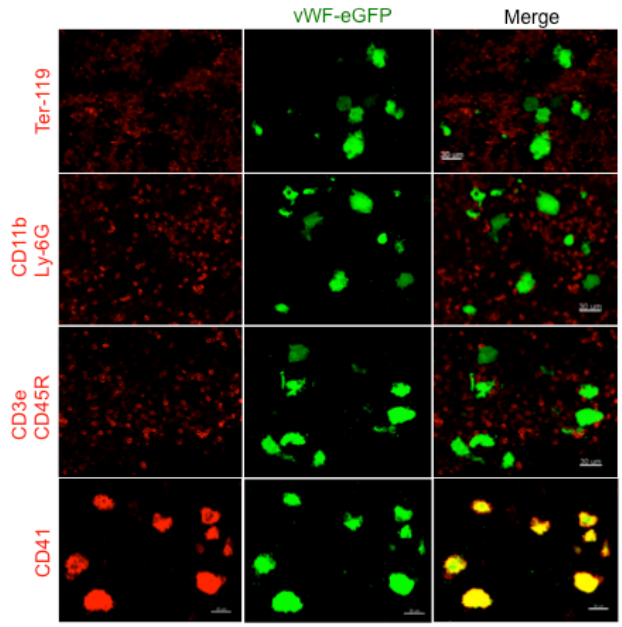

Figure 2.2.1.3 Immunostaining of erythrocytes (Ter-119), granulocytes (CD11b, Ly-6G) and lymphocytes (CD3e, CD45R), megakaryocytes (CD41) in the bone marrow of vWF-eGFP mouse. Scale bar= 30μm. [Figure and legend, Dissertation Wenwen Fu, LMU, 2017]

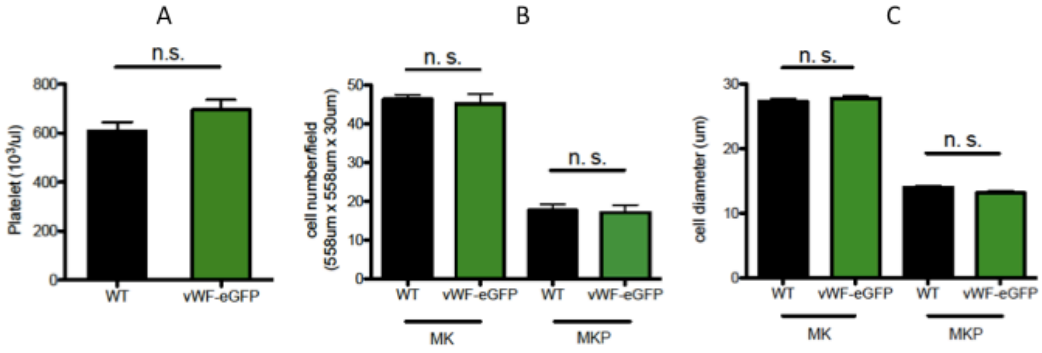

Figure 2.2.1.4 The number and size of MKs and MKps, and the number of platelets in wide type mice (WT) and vEF-eGFP mice. (A) Platelet numbers in peripheral blood. (B) MK and MKp numbers in the bone marrow. (C) MK and MKp diameters in the bone marrow. unpaired t-test. Error bar=SEM. n. s. = no significance. [Figure and legend, Dissertation Wenwen Fu, LMU, 2017]

2.2.2 PF4-cre CXCL12 flox mouse model

Platelet factor 4 (PF4) is a chemokine protein, with 70 amino acid, released from activated platelets[122]. Except promoting the blood coagulation, it has been reported that PF4 help to repair the wound [123]. Through combining with the CXCR3[124], PF4 can trigger chemo-attraction to neutrophils and monocytes, which suggests us that it might associate with the inflammatory reaction[125]. Cre-lox recombination is a technology which has been widely used to delete or express genes at specific positions of DNA[126][127][128]. In the PF4-cre+CXCL12 flox/flox mouse strain, the CXCL12 will be selectively deleted from platelets and MKs. This makes it a good model to explore the function of MK secreted SDF1. In our preliminary experiment, we found that the CXCL12 gene expression in Cre+ mice is much lower than that in Cre- mice (Figure 2.2.2.1). Through the platelet counts in the blood we found that the platelet number in Cre+ mice has no statistical significance compared to Cre- mice (Figure 2.2.2.2 A). In order to check the effect of CXCL12 knockout on the platelet recovering, we injected the mice with platelet depletion antibody. The result showed that there is no significant difference in the platelet recovery trend between the two groups. We then tested the ability of platelet migration to confirm whether the knockout of CXCL12 will affect the function of platelet or not. The data suggested that the migrated platelets fraction in Cre+ mice has no statistical significance compared to that in Cre- mice (Figure 2.2.2.3). From our FACs analysis of MK fraction in the

bone marrow we were unable to see any significant difference in the two groups (Figure 2.2.2.4).

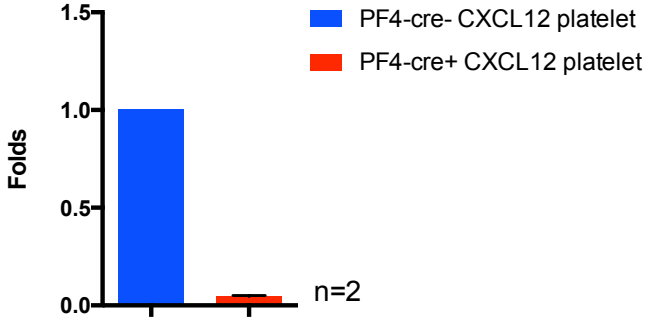

Figure. 2.2.2.1 SDF1 gene expression in platelets of PF4-cre CXCL12 mice. The data showed that the CXCL12 gene is significantly knocked out in the PF4-cre+CXCL12 mice.

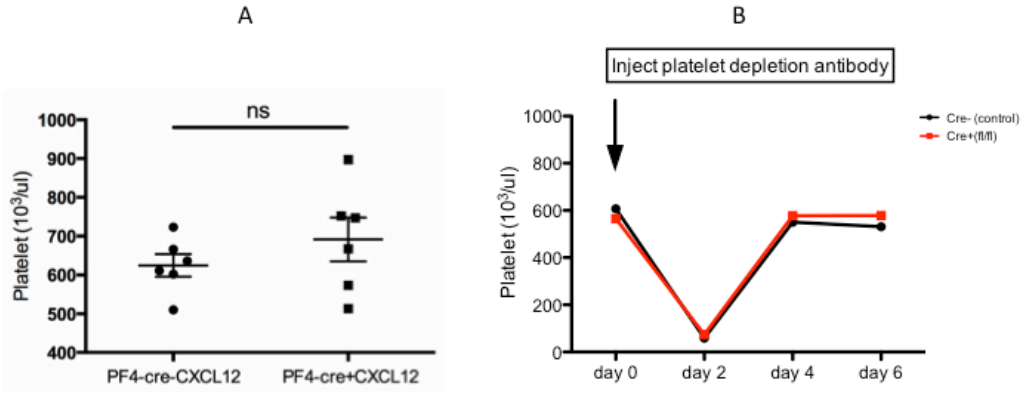

Figure. 2.2.2.2 Platelet number and function test in PF4-cre CXCL12 mice. A. Platelet measurement in PF4-cre CXCL12 mice (n=6). There is no statistical significance in platelet counts between the two groups. unpaired t-test is used. Error bar=SEM. B. Platelet measurement in PF4-cre CXCL12 mice under platelet depletion (n=3). The platelet recovery trend has no statistical significance between the two groups. Repeated measures ANOVA is used. Error bar= SEM.

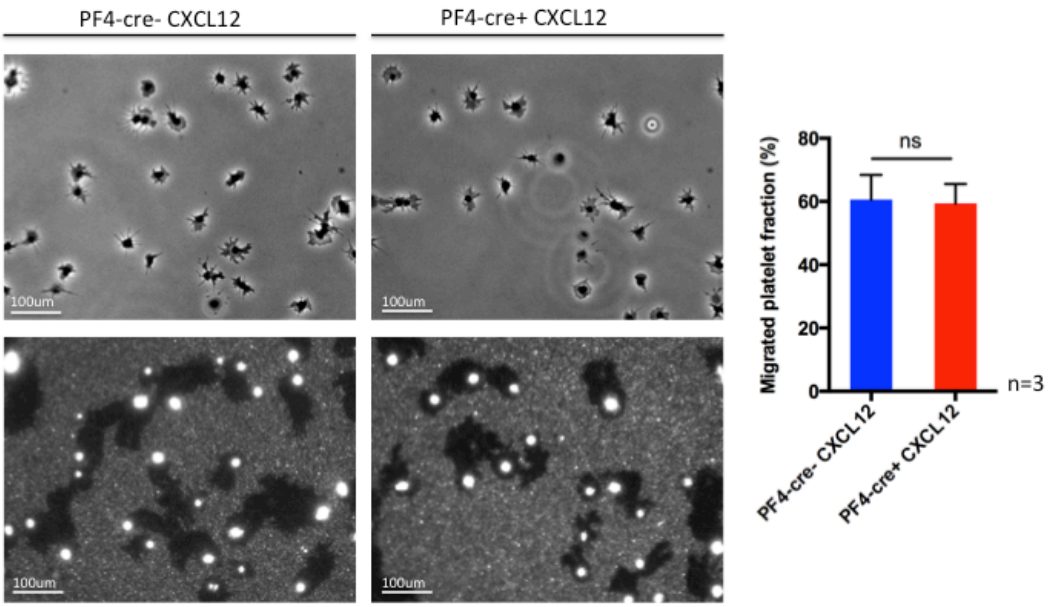

Figure. 2.2.2.3 Platelet migration experiment in PF4-cre CXCL12 mice. The fraction of migrated platelet in the Cre+ mice has no statistical difference compared to that in the Cre- mice (n=3). unpaired t-test is used. Error bar= SEM.

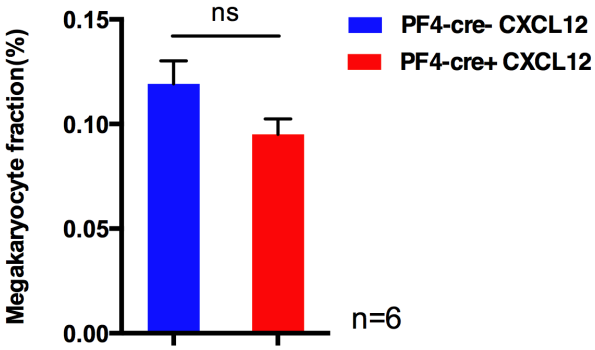

2.2.2.4 Megakaryocyte fraction in the bone marrow of PF4-cre CXCL12 mice. The MK fraction in the bone marrow in Cre+ mice has no statistical significance in comparison with that in Cre- mice (n=6). unpaired t-test is used. Error bar= SEM.

2.3 Megakaryocyte culture

Mice were treated with rmTPO (ImmunoTools, Friesoythe, Germany) with a dose of 8ng/g/day intraperitoneally in three sequential days. To isolate the bone

marrow from long bones like femurs, tibiae, and humerus, both sides of the bones were cut and the bone marrow was flushed out with 0.5% fetal calf serum (FCS) in PBS with a 26-Gauge needle. Spines were cut in cross direction and plastic pistons of the syringe were used to smash the bones to extrude the bone marrow out.

Cells were further flushed with 20-Gauge needles and were filtered with a 70um cell strainer (Miltenyl Bioec GmbH, Bergisch Gladbach, Germany). We centrifuged the cells with 300g, 4℃, 10min. We then re-suspended the pellet in 3-5ml 1×erythroid-lysis buffer for 5min at 4°C. We diluted the EDTA (Sigma Aldrich, Saint Luis, MO, USA) to the concentration of 2mM with 0.2% FCS in PBS and 30 ml of the liquid was added to terminate the reaction. The cells were centrifuged with 300g, 10min at 4°C. Cells were re-suspended in 1ml PBS and filtered with 70 um cell strainer. Then we harvested the cells and carefully transferred them into a 50ml-Falcon that contained with 9ml Easycoll separating solution (Biochrom, Germany). We centrifuged the cells with 300g, 4℃, 5min. The first 4ml of liquid were aspirated and washed with 30ml PBS. The cells were centrifuged with 300g, 4℃, 10min. The supernatant were discarded and then the pellet was re-suspended in 1ml PBS.

Cells were counted and seeded at a density of $1x10^7$ cells/well into a 6-well plate that contained with 2ml Dulbecco's Modified Eagle Medium (DMEM; Sigma-Aldrich, Merck, Germany) supplemented with 10% FCS and 1% Penicillin-Streptomycin (Thermo Fisher, San Diego, USA) in the presence of 100ng/ml

rmTPO (ImmunoTools, Friesoythe, Germany), 100ng/ml IL6 (ImmunoTools, Friesoythe, Germany) and 300ug/ml transferrin (Sigmal Aldrich, Merck, Germany)[129] for 14 days in humidified 5% CO2/95% air incubator at 37°C to obtain mature megakaryocytes. Mature megakaryocytes were enriched by bovine serum albumin (BSA) (Sigmal Aldrich, Merck, Germany) gradient.

The BSA step gradient was prepared by placing 3ml PBS on top, 3ml 1.5% BSA in PBS in the middle layer and 3ml 3% BSA in PBS in the lower layer. Cells were loaded very gently on top of the gradient and stood for 20 minutes at room temperature. Mature megakaryocytes then formed white precipitation at the bottom of Falcon. The BSA gradient process could be repeated twice to get more purified megakaryocytes.

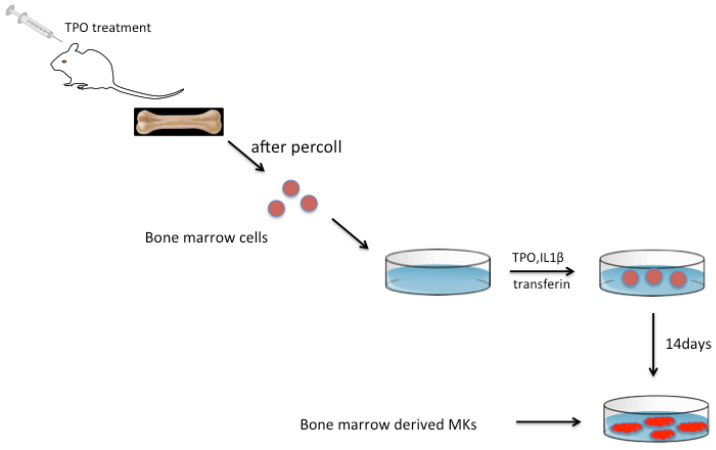

Figure 2.3 The brief process of megakaryocyte culturing.

2.4 Megakaryocyte polyploidy experiment and cell fraction test

The bone marrow derived MKs were collected after 14 days culturing. We centrifuged the cells with 300g for 5min at 4℃ and discarded the supernatant.

Cells were re-suspended in 50ul 1% BSA which was contained with 1ul CD41-FITC antibody and 1ul CD42d-APC, then we incubated the cells for 1 hour at 4℃. Cells were washed with 5ml PBS and centrifuged again with 300g, 10 min, 4℃. We discarded the supernatant and re-suspended the cells in 0.5ml PBS. Very slowly, 0.5ml 1% paraformaldehyde (PFA, Pierce, Bonn, Germany) was added into the cells. Then we incubated the sample on ice for 10 minutes. The washing process was then repeated and cells were re-suspended with 500ul DNA staining buffer (1×PBS + 2mM $MgCl_2$ + 0.05% Saponin + 0.01mg/ml PI + 10U/ml RNase A) overnight at 4℃.

We tested the MK polyploidization with flow cytometer (Beckman Coulter, Gallios Flow Cytometer 773231AD). Figure 2.4 showed the gating set in every channel. First we should set the gate on single cells (Figure 2.4 A and B). Then the gate was set on CD41+cells and expressed in histogram. As can be seen, there were two peaks that can be interpreted as positive and negative peaks (Figure 2.4 C). We then gated CD42d+ cells from the CD41+ cells that expressed also in histogram (Figure 2.4 D). At last we chose the PI staining channel and different DNA content was showed.

To test the MKs fraction in the bone marrow, we firstly isolated the cells from bone marrow following the same method as we described in the MK culturing. Instead of conducting the Easycoll separation step, we aspirate 99ul liquid and stained the cells with CD41-FITC (1:100 in dilution) and CD42d-APC (1:100 in dilution) for 25 minutes at 4℃ in dark. Then we re-suspended the cells with 3ml

PBS and centrifuged the cells with 300g for 5min at 4℃. The supernatant was discarded and cells were re-suspended with 400ul PBS. After that we tested MK fraction with Flow cytometer.

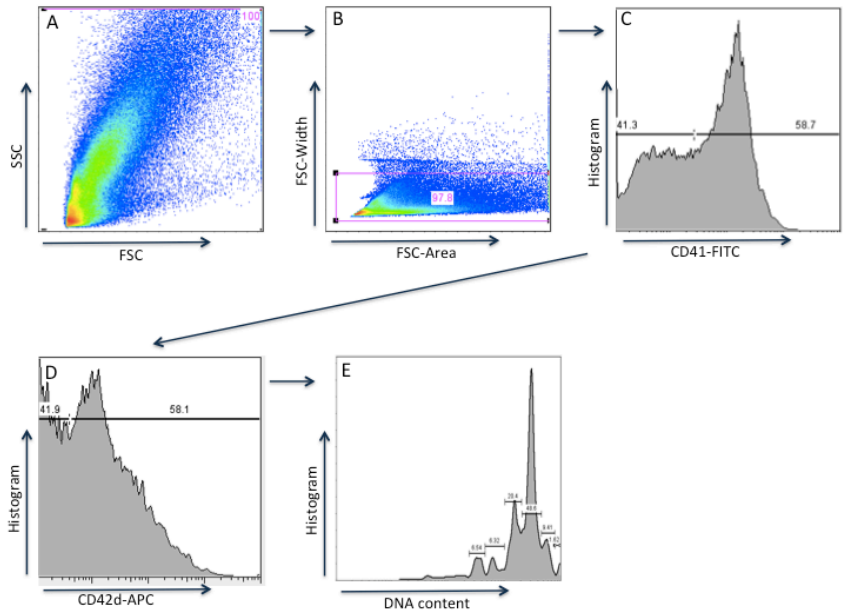

Figure 2.4 MK ploidy FACs gating process. A. Gating all of the cells; B. Gating the single cells; C. Gating the CD41+cells; D. Gating the CD42+ cells; E. Cell DNA content.

2.5 Quantitative RT-PCR

MKs RNA was isolated with the RNeasy mini kit (Qiagen, Hilden, Germany) and quantified with NanoDrop™ 2000/2000c Spektralphotometer (Thermo Fisher, MA, USA). We prepared the 2×Reverse Transcription Master Mix following the kit instruction (High Capacity cDNA Reverse Transcription Kit, Applied Biosystems) and added up to 2ug of total RNA per 20ul reaction to perform the reverse transcription with GeneAmp® PCR System 9700 (Applied Bisosystems). The primer concentration was normalized and gene-specific forward and reverse primer pair were mixed following the protocol of SsoAdanced™

Universal SYBER Green Supermix (Bio Rad, Hercules, CA, USA). We then set up the experiment and the following PCR program on Sequence MyiQ Single-Color Real-Time PCR Detection System (Bio Rad, Hercules, CA, USA). Ct values were calculated with the MyiQ Optical System software (Hercules, California, USA). And we calculated the value followed the formula $2^{\triangle Ct}$, which the $\triangle Ct$ value is calculated by formula $\triangle Ct=Ct_{GAPDH}-Ct_{SDF1}$. When PCR reaction was finished, we removed the tubes out from the machine. The PCR specificity was examined by 2% agarose gel using 20 μl from each reaction. Primers sequences of SDF1 and GAPDH were as follows:

SDF1-Fr: GCATCAGTGACGGTAAACCAG; SDF1-Rv: GTTGTTGTTCTTCAGCCGTGC

GAPDH-Fr: TCTTGGGCTACACTGAGGAC; GAPDH-Rv: ACCAGGAAATGAGCTTGACA

2.6 Immunostaining

Megakaryocytes were seeded on coverslips coated with 100ug/ml fibrinogen (Thermo Fisher Invitrogen, MA, USA) and fixed with 1% paraformaldehyde (Pierce, Bonn, Germany) for 10min at room temperature. For the staining of bone marrow (BM) tissue, we used serial frozen sections of 8um in thickness. We then washed the samples with PBS 3 times for 5 min each. The samples were blocked with the blocking solution (4.5 ml 3% BSA, 0.025g Saponin, 0.5 ml goat serum).

We then incubated the samples with different primary antibodies overnight at 4 °C or 2 hours at room temperature. Samples were washed with 1×TBST 3 times, 5min each. We then stained the samples with secondary antibodies which were mixed with Hochest (1:1000) at room temperature for 1 hour. We repeated the washing procedure. Then the samples were mounted with mounting medium (DAKO, Harmberg, Germany). Antibodies included mouse anti-mouse SDF1 in 1:50 dilution in the blocking solution (R&D Systems, Minneapolis, USA), Rat anti-mouse CD41 in 1:100 dilution in the blocking solution (ebioscience), Armenia Hamster anti-mouse CD42d in 1:100 dilution in the blocking solution, Goat anti-rat Alexa-488 in 1:100 dilution in PBS, Goat anti-rat Alexa-594 in 1:100 dilution in PBS, Goat anti hamster Alexa-488 in 1:100 dilution in PBS and Hochest nucleic acid stain (Thermo Fisher Invitrogen, MA, USA). The samples were scanned with Zeiss Microscopy equipped with 20×objective lens (Numerical Aperture=0.45), 40×objective lens (Numerical Aperture=0.65) or 63×objective lens (oil) (Numerical Aperture=1.4) and commercial CCD camera (Axiocam, CarlZeiss, Göttingen, Germany). Images were acquired by Axiovision software (CarlZeiss, Göttingen, Germany). To quantify the number of MKs, we counted the total number of MKs in four randomly selected 20×microscopic fields each coverslip.

2.7 Western blot

We harvested megakaryocytes after two times of BSA gradient and washed the cells with 1×PBS. Then samples were centrifuged with 300g, 10 min, 4 ˚C. We discarded the PBS and put cells on ice. 350ul 1×RIPA buffer (Thermo Fisher Scientific, MA, USA) was added to lyse the MKs to extract the protein. Cells were incubated on ice for 5 min. We centrifuged the cells with 14,000 g for 15 minutes at 4 ˚C to pellet the cell debris. Supernatant that contained soluble proteins was transferred to new tubes on ice. The Pierce™ BCA Protein Assay Reagent Kit was used following the manuals supplied to perform the protein quantification. Then read absorption at 562nm with GENiosTM plate reader machine (TECAN). We added 1/3 the volume of sample Nupage LDS sample buffer (4x) (Thermo Fisher Scientific, MA, USA) to the samples and then vibrated the sample evenly with the vortex and heated it for10min at 70 ˚C.

Equal amounts of protein (20ug) were separated in NuPAGE 12 % Bis-Tris gel with Running buffer MES (Novex, Thermo Fisher Scientific, MA, USA) for a constant 200 V for 50 min. Then we started to transfer the protein onto a 0.2 μm Nitrocellulose Pre-Cut blotting membrane (Thermo Fisher Scientific, MA, USA) in an X Cell SureLock™ Mini-Cell and XCell II™ Blot Module (Thermo Fisher Scientific, MA, USA) with a constant voltage 30V for 60 min. The membrane were blocked in 5% dry milk (dilute in TBST) for 30 min RT, and then we incubated it with the rabbit anti-mouse SDF1 antibody (Cell Signaling Technology, MA, USA) in 5% BSA (dilute with TBST) buffer diluted in 1:1000, and anti-GAPDH antibody

diluted in 1:10000. We put the falcon that contained the membrane on a shaker at 4°C overnight/12h. After that we washed the membrane with TBST in 3 times, 5 min per time. The membrane was incubated with the corresponding horseradish peroxidase (HRP)-conjugated secondary antibody (dilution 1:1000) for 1 hour at room temperature with shaking. We repeated the washing process with TBST for 3 times. Equal volumes of Amersham ECL™ Prime Western Blotting detection reagent A & B (GE Healthcare, Chicago, Illinois, USA) were mixed. We put the membrane in a small clean plate and added the detection reagent and incubated for 5 min at room temperature. We drained off the detection reagent and put the membrane on a new clear plastic bag. Air bubbles must be removed. The membranes were exposed to FujiFilm X-ray (FUJI Film corporation, Tokyo, Japan) for 5 min.

2.8 Megakaryocyte progenitor FACs analysis

MKps abundant cells were harvested after the percoll, which was in the same procedure as we described in MKs culturing. The cells were stained with the Pacific Blue anti-mouse TER-119/Erythroid, anti-mouse Ly-6G/Ly-6C (Gr-1), anti-mouse/human CD11b, anti-mouse CD3, anti-mouse CD8a with 3:1000 in dilution, PE/Cy7 anti-mouse Ly-6A/E (Sca-1) Antibody with 2.5:1000 in dilution, APC anti-mouse CD117 (c-Kit) Antibody with 5:1000 in dilution, CD41-FITC anti-mouse with 1:100 in dilution at 4°C. The megakaryocyte progenitors were identified by forward and side scatter plotting and Lineage (-) Scal1 (-) C-kit (+)

CD41 (+) gating. To analyze the MKps in vWF-eGFP mice, cells were stained only with PB-Lineage, PE/Cy7-Scal1 and APC-C-kit antibodies but without the CD41-FITC staining. The eGFP signal was detected in the same channel as FITC (Figure 2.8).

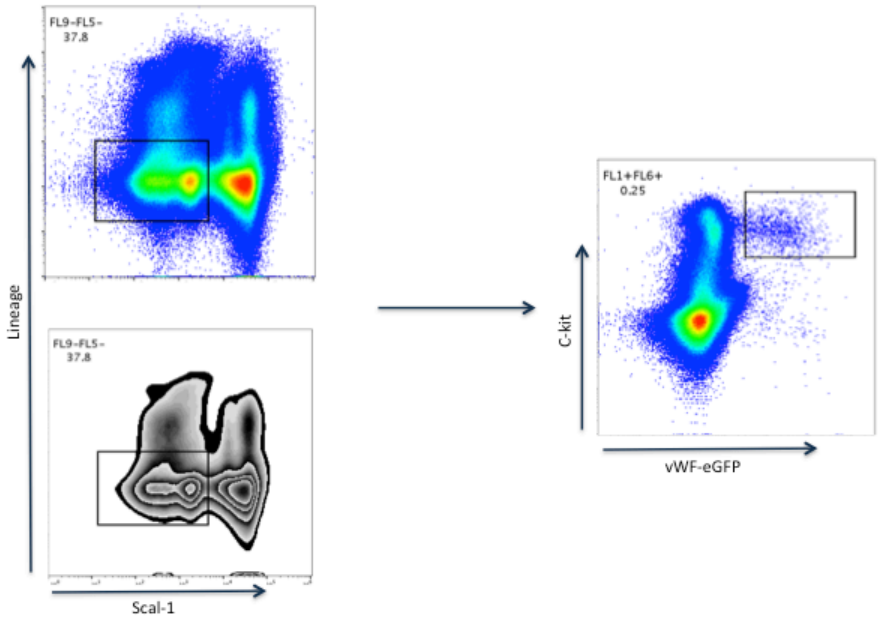

Figure 2.8 FACs protocol of MKps from vWF-eGFP mice. After forward and side scatter we gating the single cells out. And then following this protocol we gating the Lineage/Scal-1 double negative cells out and setting the gate on the c-kit/vWF double positive cells.

2.9 Two-photon whole-mount imaging of the bone marrow

Preparations of whole-mount tissues: After the mice were anesthetized, cutting off the postcava, and then flushing the blood out by injecting the mice with 3ml PBS from the apex of the heart. Via injecting 3ml 4% paraformaldehyde (PFA) into the left ventricle through the apex of the heart, the tissues were fixed. Then the sternum and fermoral or tibial bones were isolated and soaked in 4%PFA for

30 min. Bones were incubated in 15% sucrose for 2 hours and later 30% sucrose overnight (or more than 8h) at 4°C. Later the bones were embedded in Tissue-Tek® OCT and put in liquid nitrogen and 2-Methylbutane (Isopentane, Sigma-Alrich, Saint Louis, MO, USA) to be frozen. The samples were used at least 2h after storing in an-80°C ice fridge. The bones were carefully shaved on Histo Serve NX70 cryostat (Celle, Germany) until the bone marrow cavity was fully exposed. Carefully harvested the bones from the melting OCT, then blocking the sternum with 10% goat serum (NGS, Thermo Fisher Scientific, Massachusetts, USA) and 0.5% Triton X-100 (Sigma-Alrich, Saint Louis, MO, USA) at room temperature for 2 hours. We incubated the bones directly with primary CD144 rat anti-mouse antibody (1:100 dilution in 1×PBS) and CD42d Armenia hamster anti-mouse antibody (1:100 dilution in 1×PBS) at room temperature overnight or 12h. The sternum was washed gently in 1×PBS and incubated with the goat anti-hamster Alexa Fluor 647 (1:100 dilution in 1×PBS) and goat anti-rat Alexa Fluor 594 (1:100 dilution in 1×PBS) at room temperature for 2h. We repeated the washing procedure and the bones were incubated with CD41-FITC (1:100 dilution in 1×PBS) at room temperature for 4 hours. Images were acquired by using intravital 2-photon (LaVision Biotech, Bielefeld, Germany).

To scan the bones from C57Bl/6J mice, 800nm was used as an excitation wavelength. Photomultiplier values were as followed: Red-65, Blue-70, Green-58, near Infrared (NIR)-65. Single images were acquired in depth of 50-80μm, with

z-interval of 2μm. After that the images were reconstructed in three dimensions with the XuvTools software and Imaris software (Bitplane, USA).

We quantified the number of MKs and MKps in the whole mosaic image, which all of the cells had been normalized by the volume of bone marrow in the image. The number of MKs and MKps were measured by counting directly. The distance from cells (MKs and MKps) to vessels was also quantified.

2.10 Platelet and neutrophil measurement

The mice were kept in a container and only the tail was pulled out. 100ul 1:7-anticoagulant citrate dextrose solution whole blood was collected from the tail vein. The blood cells were measured with the blood cell counter machine (ABX Micros ES 60, HORIBA, Kyoto, Japan). 2ul blood was aspirated into 98ul PBS and the platelets were stained with 1ul CD42d-APC for 25min at room temperature. Up to 400ul platelets were re-suspended and 4ul cell counting beads were added in. FACs test was performed directly. After the Flowjo analysis, we got the platelet number that tested by the FACs. With the formula $4\times 10^4/500=2C/N$ we managed to get the platelet concentration in peripheral blood. Here the “C” stands by the concentration of platelet in the blood and “N” stands by the platelet number tested by FACs.

We next aspirated the left 98ul blood and incubated with 1×erythroid lysis buffer for 5min at room temperature. Cells were centrifuged with 300g, 5min, 4 °C. We repeated this process if there were a lot of red cells in the precipitation.

We then stained the cells with 2ul PE-Ly6G (Biolegend, San Diego, CA, USA) for 25 min, 4 °C. FACs was performed with the flow cytometer (Beckman Coulter, Gallios Flow Cytometer 773231AD) and analyzed the data with Flowjo. After we got the fraction of neutrophils, we multiplied this number by the WBC cell number that we got from the blood cell counter machine, which was the neutrophils number in the blood.

2.11 Lineage depletion experiment

Bone marrow cells were flushed out with PBS + 2% FCS through 26-Gauge needle. We kept flushing the bone marrow with 20-Gauge needle until it smashed into single cells. Cells were filtered with a 70μm cell strainer (Miltenyl Bioec GmbH, Bergisch Gladbach, Germany) and centrifuged with 300g, 10 min, 4°C. 3-5ml 1×erythroid lysis buffer were added into the precipitation and incubated for 5min at 4°C. 30ml 2% EDTA (Sigma Aldrich, Sant Luis, MO, USA) were added to stop the reaction and were centrifuged with 300g, 10min at 4°C. Cells were re-suspended in 1ml 0.5% BSA in PBS and filtered with 70 um cell strainer. We counted cells and lineage cells were depleted followed the lineage cell depletion kit (Miltenyl Bioec GmbH, Bergisch Gladbach, Germany) protocols. The protocols were as follows: we added Biotin cocktail antibody to the precipitation in 10ul/10^7 cells and incubated the cells at 4°C for 10 min. Then we added 2%EDTA+0.5%FCS in 30ul/10^7 cells and micro-beads in 20ul/10^7 cells and incubated them for 15min at 4°C. 2ml 2%EDTA+0.5%FCS were used to wash

the cells and centrifuge 10min with 300g at 4°C to harvest the cells. Cells were re-suspended with 2ml 2%EDTA+0.5%FCS and were moved into a FACS tube that stood in the magnetic field of a suitable MACS Separator for 10min, room temperature. The liquids were then dropped slightly (ensuring that they were not shaken) into a Falcon that contained with 30ml 2%EDTA+0.5%FBS and cells were centrifuged again with 300g at 4°C for 10 min. Then we counted the cells for use. In the MKps sorting experiment, we stained the Pacific Blue anti-mouse TER-119/Erythroid, anti-mouse Ly-6G/Ly-6C (Gr-1), anti-mouse/human CD11b, anti-mouse CD3, anti-mouse CD8a with 0.2ul/10^6 cell in dilution, PE/Cy7 anti-mouse Ly-6A/E (Sca-1) Antibody with 3ul/10^6 cell in dilution, APC anti-mouse CD117 (c-Kit) Antibody with 3ul/10^6 cell in dilution, CD41-FITC anti-mouse with 2ul/10^6 cell in dilution and the final PI concentration of 5ug/ml at 4°C. The flow cytometry sorting experiment was performed with MoFlo Astrios EQ (Beckman Coulter Life Sciences, CA, USA) machine with a 100 um diameter nozzle.

2.12 Cell trans-migration experiment

The first step was to prepare SDF1 gradients. 0.6ul 100ng/ul SDF1 (ImmunoTools, Friesoythe, Germany) were added into 599.4ul serum free DMEM in the 24-well plate. We added 2x10^4 MKs into the 24-well plate that coated with 100ng/ml fibrinogen. We used a cell number of 2x10^4 MKs which was the most suitable because it allowed all of the MKs to spread evenly on the

bottom; a higher cell number would have been too crowded for the MKs to spread. After about 6h, most of the MKs were able to adhere to the fibrinogen stably. Then we pre-infiltrated the 5um pore size transwell inserts (Corning, New York ,USA) with serum free DMEM at least 2 hours at 37°C.

The isolated BM cells were incubated with 1×erythroid-lysis buffer. After terminating the reaction with 30ml 2% EDTA (Sigma Aldrich, Sant Luis, MO, USA) we then centrifuged the cells with 300g at 4°C for 10 min. Cells were re-suspended in 1ml PBS and filtered the cells with 70um cell strainer. Then we slowly added the cells into a 50ml Falcon that contained with 9ml easycoll. Cells were centrifuged at 300g, 4℃, 5min. We aspirated the first 4ml liquids and washed them with 30ml PBS. Cells were centrifuged with 300g, 4℃, 10min. Cells were re-suspended in 1ml PBS. We aspirated 100ul cells into a FACs tube and stained them following the MKps FACs protocol. After the analysis on the Flowjo (FlowJo LLC, Oregon, USA), the fraction of MKps was calculated. We put up to 10^4 MKps (liquid volume should be less than 200ul) in the 5.0 um pore transwell inserts (Corning, USA) that stood in the 24 wells-plate and cultured for 10 hours in humidified 5% CO2/95% air incubator at 37°C.

As to the migrated cells harvest, we first took out the transwell inserts carefully and aspirated the liquids from the well into the FACs tubes. Every well will be washed 3 times, with 1ml PBS each time and we checked the plate under microscopy to make sure that most of the cells have been harvested. We then

centrifuged the harvested cells with 300g, 10min, 4°C. The supernatant was carefully discarded and cells were re-suspended to 100ul. We stained the cells following the MKps staining protocol and incubated them for 25 min at 4°C in dark. Cells were re-suspended to 400ul with PBS and cell-counting beads were added (vibrating before using) at the concentration 1ul beads/100ul liquid (Thermo Fisher, MA, USA). At last, cells were analyzed with flow cytometer.

2.13 Statistical analysis

All data is presented as means±SEM. Student's unpaired t-test and repeated measures ANOVA are used in this study as the statistical methods. P values of less than 0.05 are considered as statistical significant.

3. Results

3.1 Bone marrow derived megakaryocyte isolation and purity of megakaryocyte

After 14 days culturing, the mature megakaryocytes derived from the bone marrow of wild-type mice were harvested in the 6-well plate (Figure 3.1.1).

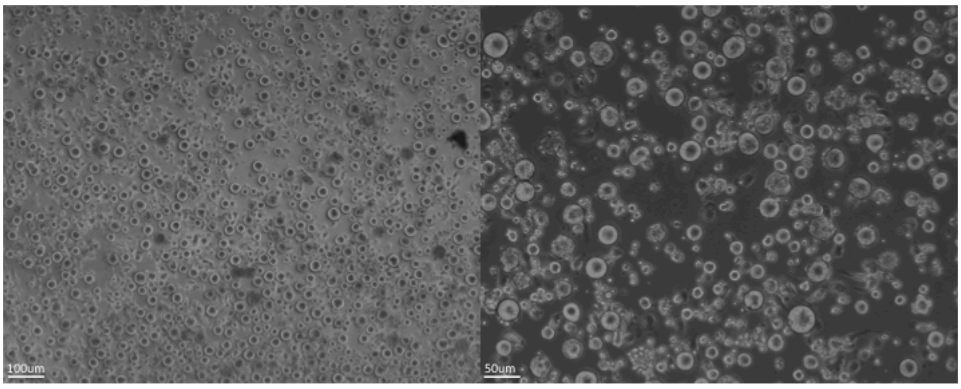

Figure. 3.1.1: The megakaryocytes after 14 days culturing. Scale bar is 100um and 50 um, respectively.

The vWF-eGFP bone marrow derived megakaryocytes were enriched after two times of BSA gradient. We randomly chose 4 different areas on each coverslips and counted in all 3 different coverslips. And here we marked MKs with CD41 (Figure 3.1.2) instead of CD42d, due to the high background staining of CD42d at the 20×focus (Figure 3.3.5). The MKs purity, calculated from the fraction of the cells (diameter≥20μm) with vWF/CD41 double positive in the CD41 single positive cells, was 92.66%. This was pure enough for us to perform the molecular biological experiment of megakaryocytes.

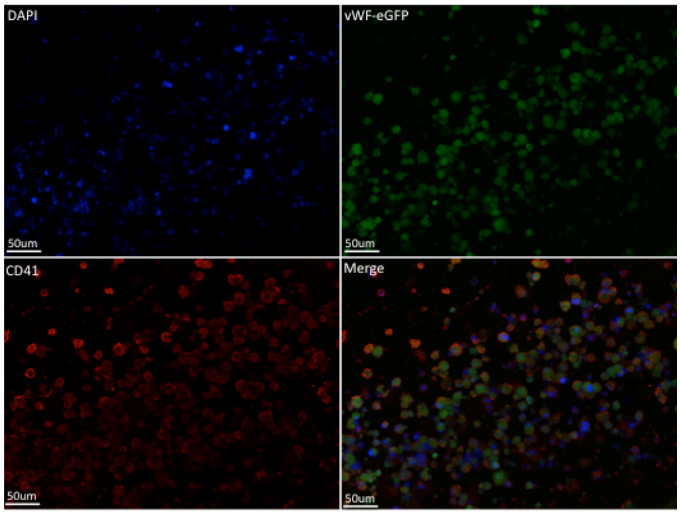

Figure. 3.1.2 Immunostaning of vWF-eGFP bone marrow derived mature megakaryocytes. Scale bar= 50 um.

3.2 The maturation of megakaryocyte

The best way to distinguish mature MKs is to test the ploidy of the cells. Normally we define those MKs which are more than octoploidy (8N) as matured [23]. Here we used the 10 days cultured MKs as a control to compare that to the ploidy of 14 days cultured MKs. The result showed that there were more mature MKs in the 14 days cultured cells (Figure 3.2). Although after 10 days culturing, most MKs were mature, the maturity of the 14 days cultured MKs were even higher. The fraction of mature MKs (the cells that have ploidy level higher than 8N) in the 14 days cultured MKs was 94.9%. This result is further evidence that the 14 days cultured MKs were mature enough to be used to investigate the SDF1 expression and so as to perform the MK-MKp trans-migration assay.

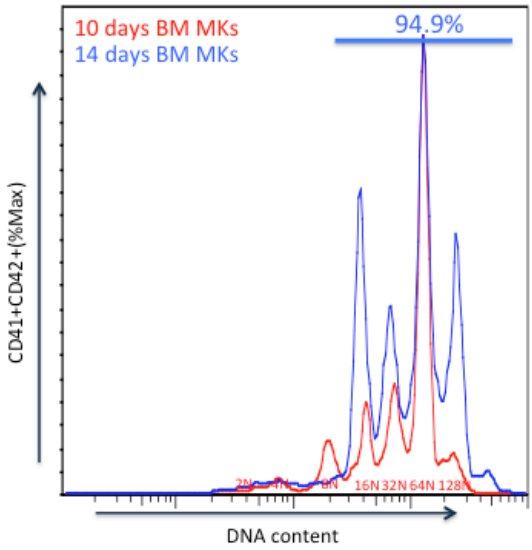

Figure 3.2 The DNA content in 10 days and 14 days cultured megakaryocytes. The blue color represents the 14 days cultured MKs and the red color represents the 10 days cultured MKs. The ploidy is measured by the mean fluorescence intensity.

3.3 The expression of SDF1 in megakaryocyte

Our RT-PCR result showed that the SDF1 gene was expressed in the bone marrow derived MKs (Figure 3.3.1). And western blot experiment showed that SDF1 is expressed in the MKs, but with a relatively low level (Figure 3.3.2).

The immnostaining of coverslips that coated with MKs also showed a positive SDF1 signal in mature MKs (Figure 3.3.3). Taken together, SDF1 was expressed in the mature bone marrow derived MKs. However, the background of SDF1 immunostaning in megakaryocytes of bone marrow section was too high to distinguish the structures (Figure 3.3.4). We then introduced the DsRed-CXCL12 mice bone marrow section (from Dresden University), in which the DsRed signal had been labeled automatically on CXCL12/SDF1. We stained the samples with both CD42d and CD41 (Figure 3.3.5). Although the CD42d staining had a high

background under 20 × focus, it was possible for us to distinguish the megakaryocytes from the cell morphology and DAPI signal. The DsRed signal in the CD42d+ cells was very weak and even nearly the same as the background. Through the CD41 staining we could find the MKs more clearly, whereas the DsRed signal in the position where MKs located was still similar to the background. All of these data suggest that the SDF1 expression in matured bone marrow derived MKs is at a low level.

The result of chemokine kit test showed that the stimuli of MK depletion on the one hand can hardly have affected the global content of SDF1 in the bone marrow (Figure 3.3.6), and on the other hand it has proved that MKs expressed a very low level of SDF1 (Figure 3.3.7). And the gravity of SDF1 in the MK depletion group was quite similar to the positive control, which means that the bone marrow contains large amounts of SDF1 (Figure 3.3.6).

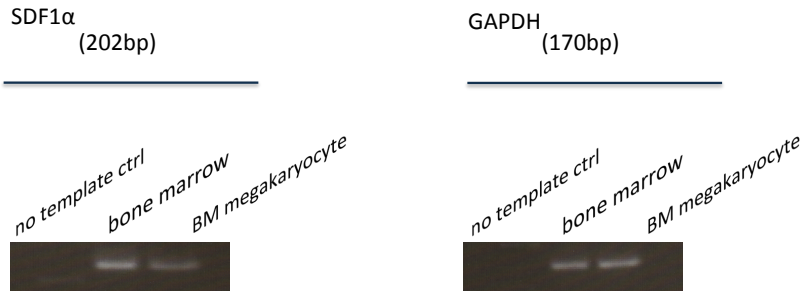

Fig. 3.3.1 The SDF1 gene expression in whole bone marrow cells and bone marrow derived MKs.

The data showed that the SDF1 gene expressed in the bone marrow derived megakaryocytes.

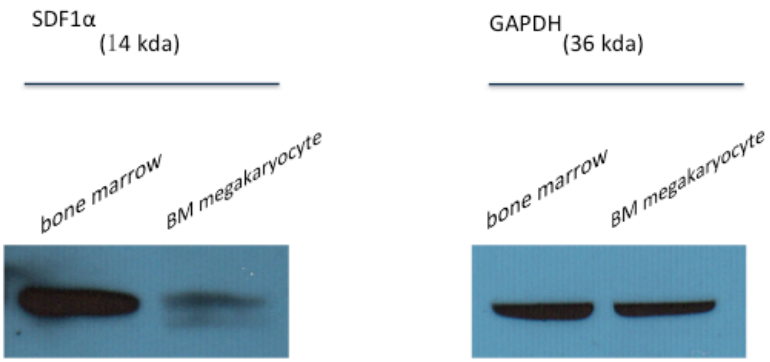

Figure. 3.3.2 SDF1 western blot experiment of whole bone marrow cells and bone marrow derived megakaryocytes. The figure clearly showed that the SDF1 expressed in the bone marrow derived MKs.

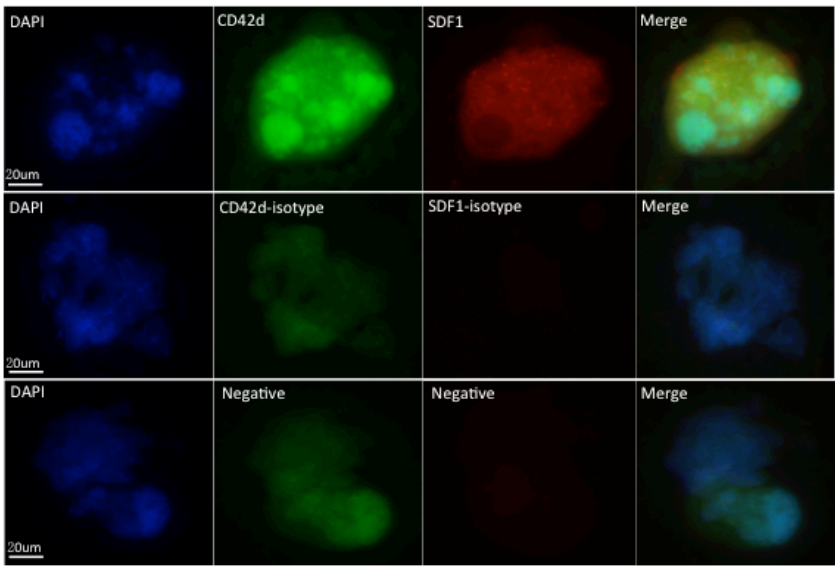

Figure.3.3.3 Immunostaining of SDF1 in bone marrow derived mature megakaryocytes. The SDF1 staining has an obvious signal in mature MKs (CD42+). Scale bar=20um.

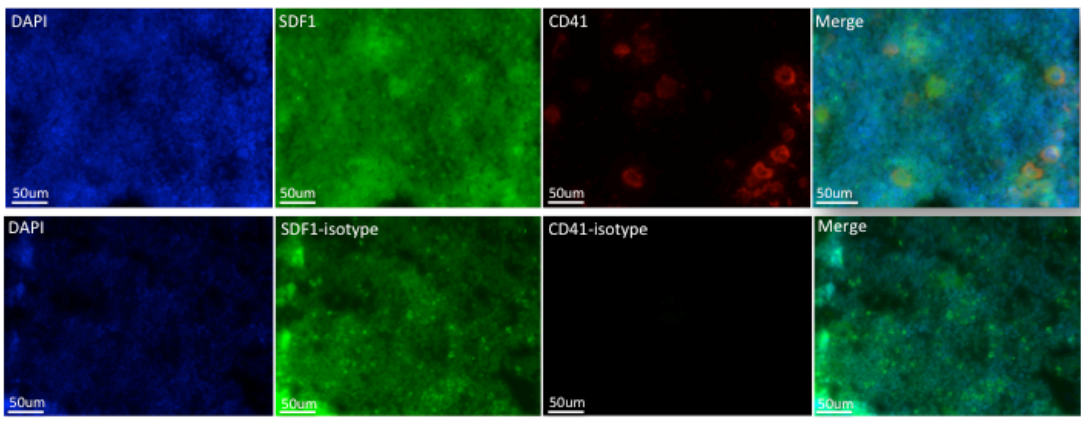

Figure.3.3.4 Immunostaining of SDF1 in bone marrow section of wild type mice. The SDF1 and its isotype staining have high background. Scale bar=50um.

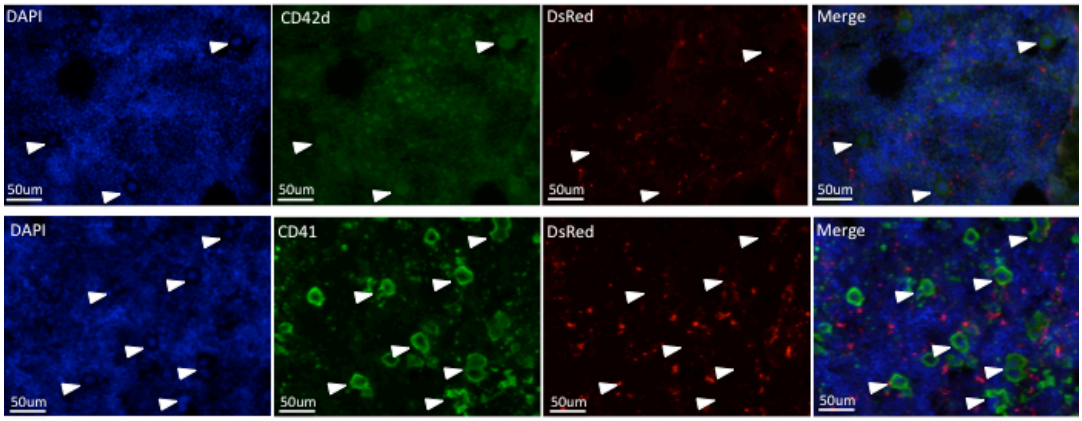

Figure. 3.3.5 Immunostaining of SDF1 in DsRed-CXCL12 mice bone marrow section. The MKs were marked with CD42d and CD41, respectively. The DsRed signal was labeled on the CXCL12 automatically. Scale bar=50um.

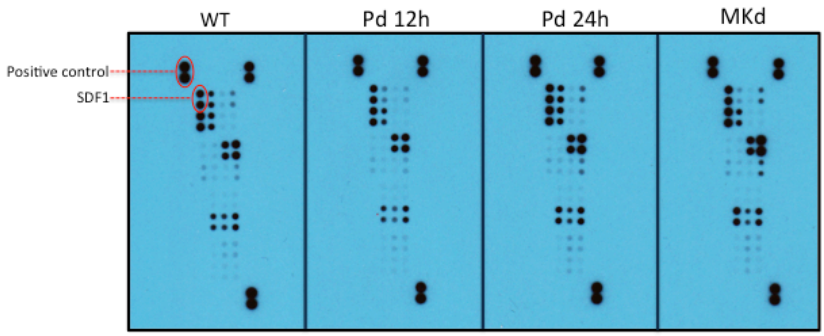

Figure. 3.3.6 The chemokine kit test of 28 different chemokines expression in the bone marrow supernatant. The bone marrow supernatant is isolated from wild type mice, 12h after platelet depletion, 2 days after platelet depletion and MK depletion mice, respectively.

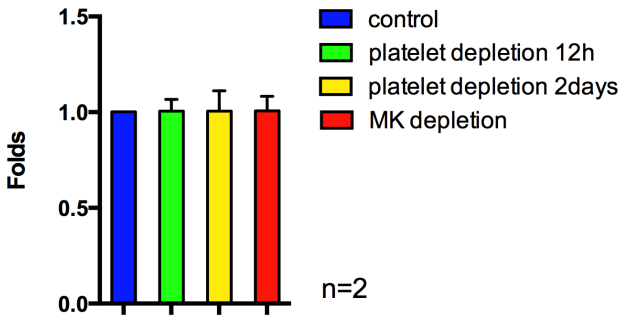

Figure. 3.3.7 The chemokine kit test of SDF1 expression in the bone marrow supernatant. The bone marrow supernatant is isolated from wild type mice, 12h after platelet depletion, 2 days after platelet depletion and MK depletion mice, respectively.

3.4 The isolation of megakaryocyte progenitors

We modified the published protocol[6] to harvest megakaryocyte progenitors. In order to get more MKps, we even isolated the bone marrow cells from the spine, from which we could get nearly 1.5-2 folds bone marrow cells than that only isolated from the limbs (humerus, tibias and femurs). However, after the linage cell depletion there were only around 10% cells left, which are MKp abundant cells. And there was only 1% target cells would be sorted from these MKps abundant cells. The cell number was far less than the MKps we need. Due to low efficiency of lineage depletion and flow cytometry cell sorting, we decided to use the percoll to isolate the MKp abundant cells[129] and performed our transwell assay. The details of cell isolation procedure have been elucidated in the part of methods and materials. In this way, we were able to get enough MKps to conduct the trans-migration assay, the MKp fraction was normally more than 0.5%. Which means that there are 10^4 MKps contained in 2×10^6 cells. We then put up to 2×10^6 cells in the transwell inserts to perform the trans-migration experiment.

3.5 In vitro effect of SDF1 to MKps

We put up to 10^4 MKps in the transwell inserts and after 10 hours incubation we

collected the cells that had migrated down to the 24-well plate to perform the FACs analysis. As it is shown in Figure 3.5, the SDF1 has a strong chemo-attraction effect on MKps. The mean number of the migrated MKps in SDF1 group is 35. It has statistical significance when compared to the control group. However, this chemo-attraction effect was inhibited after the cells were pre-incubated with CXCR4 antagonist-AMD 3100 (50ug/ml RT[130]), in which very few MKps migrated towards the SDF1 gradient. The result had no statistical significance in comparison with the control group.

Figure 3.5 The SDF1 trans-migration experiment. Every group we put in all $2x10^6$ cells that contained 10^4 MKps in a transwell insert. SDF1 can attract more MKps migrate towards it. When the cells were blocked with AMD3100, very less MKps migrated towards SDF1. *** means $p<0.001$. unpaired t-test is used. Error bar= SEM.

3.6 In vitro effect of MKs in the migration of MKps

In order to investigate whether mature megakaryocytes can direct the migration of megakaryocyte progenitors or not, we next examined the chemotaxis effect of TPO (100ng/ml), MKs and TPO (100ng/ml) treated MKs to the MKps. The trans-migration results of these three groups had no significant difference compared to the control group (Figure 3.6). And SDF1 as a positive control could

obviously direct the migration of MKps. The results had statistical significance.

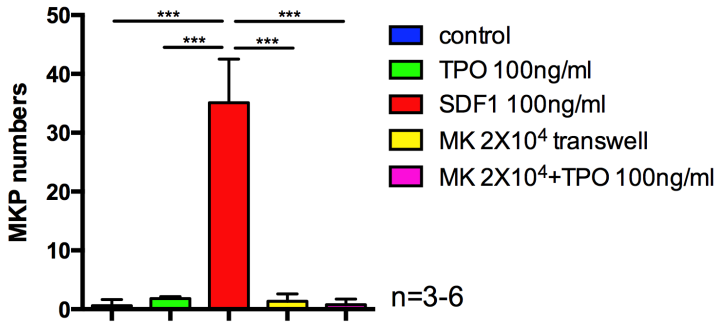

Figure 3.6 The TPO, megakaryocyte, TPO treated MK-MKp trans-migration experiment. In every group, all the $2x10^6$ cells that contained 10^4 MKps were added in a transwell insert. SDF1 had a statistical significant chemotaxis effect on the MKps. However, TPO, MKs and TPO triggered MKs could attract significantly fewer MKps，which had no statistical significance compared to the control group. *** means $p<0.001$. unpaired t-test is used. Error bar= SEM.

3.7 CXCR4 expression on MKps

Although SDF1 can attract MKps migrating towards it, the migrated cell number is much lower than the total number of MKps that we put in the transwell inserts. To investigate the reason, we tested the CXCR4 expression on MKps and found that the CXCR4 fluorescence peaks did not separate significantly from control groups (Figure 3.7.1), which means that the CXCR4 expression on MKps was in a relatively low level. However, we could distinguish the peaks of CXCR4 expression on the neutrophils easily (Figure 3.7.1). The analysis of the mean fluorescence intensity (MFI) showed that the expression level of CXCR4 among MKps and control groups is statistically significant (Figure 3.7.2)($p<0.05$). In consequence, the CXCR4 was expressed on the MKps, although at a relatively low level.

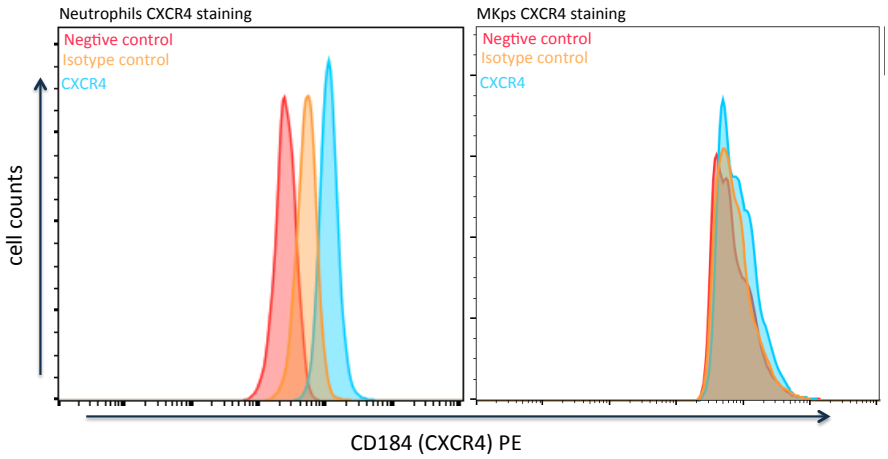

Figure 3.7.1 Flow cytometry analaysis of CXCR4 expression on neutrophils and megakaryocyte progenitors. Both of the two cells were stained with PE-conjugated antibody specific for CXCR4.

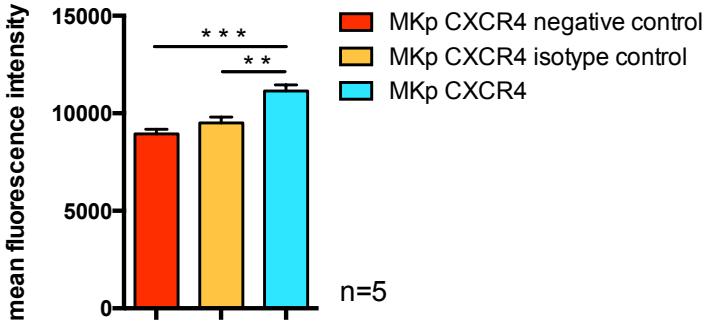

Figure 3.7.2 Mean fluorescence intensity of CXCR4 expression on MKps. The data showed us that CXCR4 is expressed on MKps. *** means p<0.001; ** means p<0.01. unpaired t-test is used. Error bar= SEM.

3.8 In vivo experiment of CXCR4 blocking (AMD 3100 treatment)

To investigate whether the CXCR4 blocking will also affect the chemo-attraction between SDF1 and MKps in situ, we then continuously injected AMD 3100 into mice subcutaneously in a dose of 1mg/kg/day[131] for 5 days. There was no significant difference in platelet counts between AMD 3100 treatment group and control group (p=0.478)(Figure 3.8.1 A). The neutrophils counts had an

increasing trend in the AMD 3100 treatment group, however, the difference was not significant (p=0.4571)(Figure 3.8.1 B).

We next analyzed the distance of MKs and MKps to the vessels in whole-mount staining which performed with 2-photon microscopy. The data showed a trend that MKs and MKps located slightly distant from the vessels. The number of MKs and MKps in AMD 3100 treatment group increased significantly in the cell-vessel distance range of 0-5 um and 5-10 um (Figure 3.8.2 A and C). We then calculated the numbers of MKs and MKps, however, the data showed no significant difference after 5 days treatment with AMD 3100 compared to the control group (Figure 3.8.2 B and D). The fraction of MKps that attached to mature MKs in AMD 3100 treatment group had no statistical significance compared to the control group (Figure 3.8.2 E).

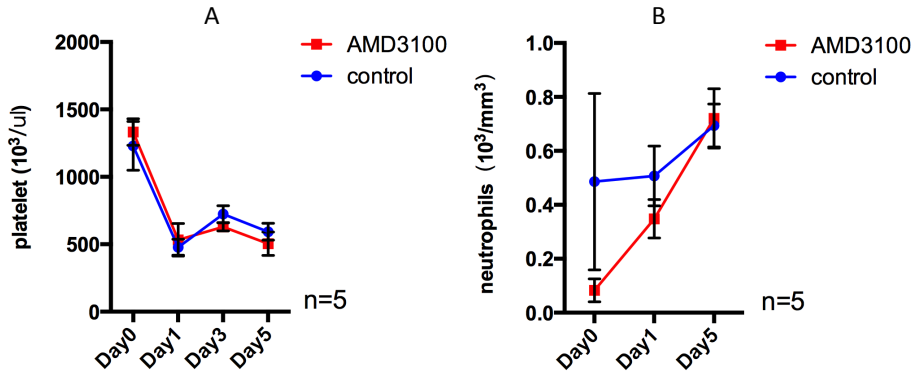

Figure 3.8.1 Platelets and neutrophils measurement of wild type mice (n=5) and AMD 3100 treated mice (n=5). (A) Platelet measurement of peripheral blood. p= 0.478. (B) The neutrophils measurement of peripheral blood. p= 0.4571. Repeated measures ANOVA is used. Error bar= SEM.

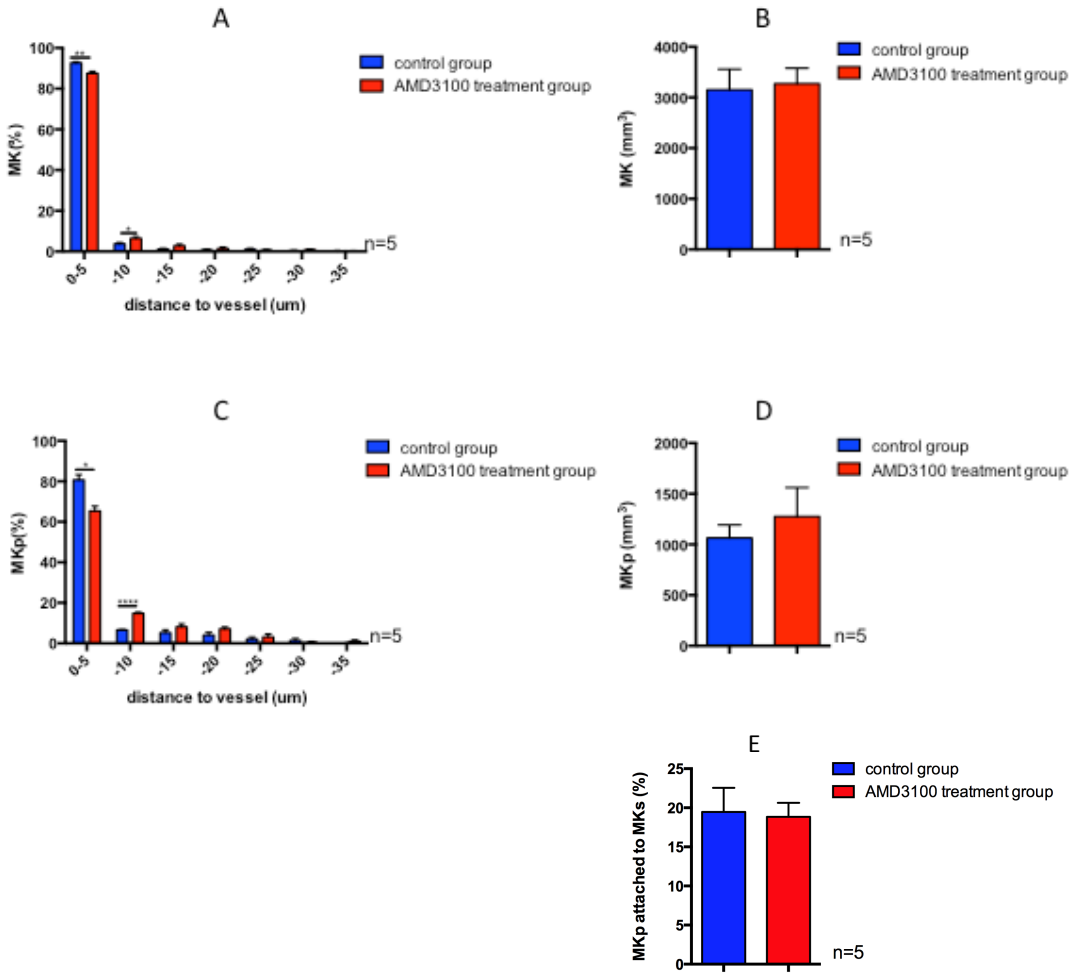

Figure 3.8.2 MK and MKp quantification in the sternum bone marrow whole-mount staining of the wild type mice (n=5) and AMD 3100 treated mice (n=5). (A) The distance of mature megakaryocytes to the vessels. (B) The number of MKs per mm^3 sternum bone marrow. (C) The distance of megakaryocyte progenitors to the vessels. (D) The number of megakaryocyte progenitors per mm^3 sternum bone marrow. (E) The fraction of megakaryocyte progenitors that attached to mature megakaryocytes. unpaired t-test is used. Error bar= SEM. * means $p<0.05$; ** means $p<0.01$; *** means $p<0.001$; **** means $p<0.0001$

Along with our analysis of the effect of AMD 3100 at stable state, we also investigated the effect of AMD 3100 on the platelet recovering when mice were under platelet depletion (PD) stimuli. Platelet measurement result showed that

the PD and AMD 3100 combination treatment group (combination group) could not significantly prevent the platelet recovering (p=0.1387) (Figure 3.8.3 A). The measurement of neutrophils in the combination group did not show a significant increasing trend compared to the control group (p=0.1227) (Figure 3.8.3 B).

Most MKs and MKps in both of the two groups stably stayed close to the vessels (Figure 3.8.4 A and C). The result had no statistical significance. The number of MKs and MKps did not change significantly in the combination group (Figure 3.8.4 B and D). The fraction of MKps that attached to mature MKs in combination group had no significant difference compared to the PD group (Figure 3.8.4 E).

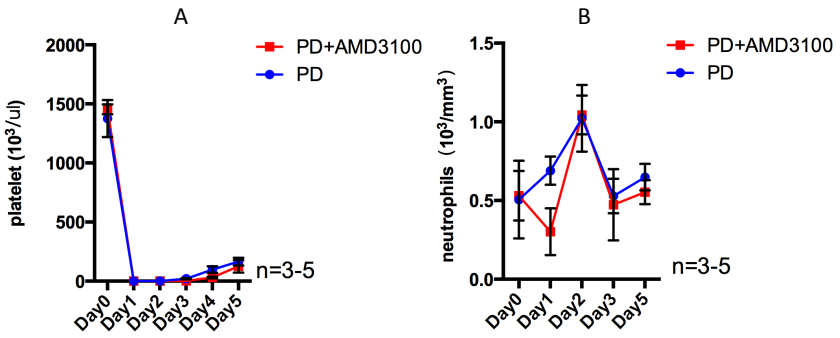

Figure 3.8.3 Platelets and neutrophils measurement of platelet depletion mice (n=5) and platelet depletion (PD) combined with AMD 3100 treated mice (n=3). (A) Platelets measurement of peripheral blood by flow cytometry. (B) The neutrophils measurement of peripheral blood. PD-platelet depletion. Repeated measures ANOVA is used. Error bar= SEM

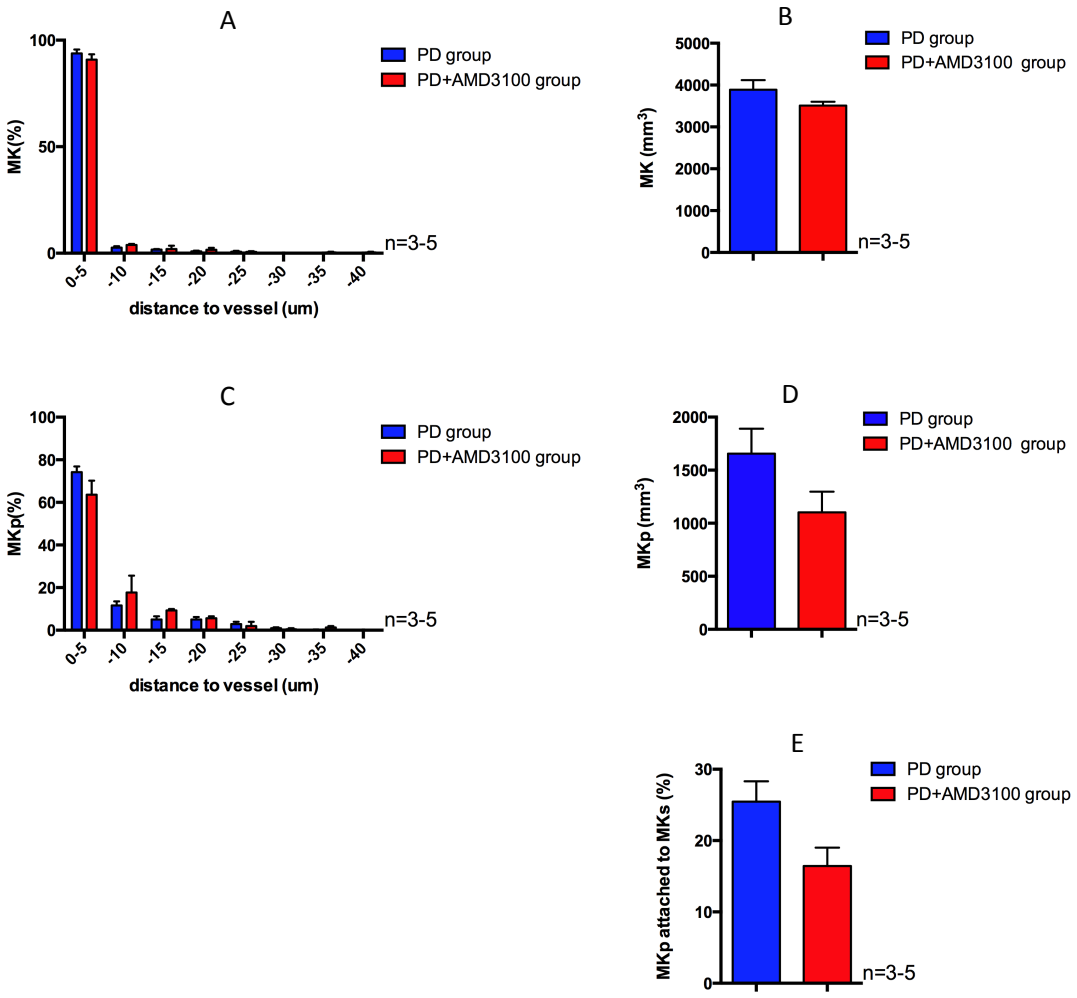

Figure 3.8.4 MK and MKp quantification in the sternum bone marrow whole-mount staining of the platelet depletion (PD) mice (n=5) and platelet depletion (PD) combined with AMD 3100 treated mice (n=3). (A) The distance of mature megakaryocytes to vessels. (B) The number of MKs per mm^3 sternum bone marrow. (C) The distance of megakaryocyte progenitors to vessels. (D) The number of MKps per mm^3 sternum bone marrow. (E) The fraction of megakaryocyte progenitors that attached to mature megakaryocytes. unpaired t-test is used, Error bar= SEM.

4. Discussion

The main findings of our study are as followed. (1) We successfully cultured the bone marrow derived megakaryocytes and confirmed the maturation of megakaryocytes through polyploidy FACs experiment. Moreover, our MKs culturing protocol enables us to isolate enough purified MKs in a more convenient way. (2) It is proven that SDF1 can be expressed by mature megakaryocytes. (3) A MK-MKp trans-migration model has been established and through this model we were able to find that both the MKs and TPO treated MKs cannot trigger the MKps migration. However, SDF1 has a chemotaxis effect on a fraction of MKps. (4) Whole-mount staining results showed us that AMD3100 can relocate MKs and MKps at the steady state. However, this effect was not so obvious when the mice were under platelet depletion.

4.1 Megakaryocyte culturing and SDF1 staining

Previous researches that focused on bone marrow derived MKs have frequently encountered issues. One major problem has been that megakaryocyte is one of the most rare cells in bone marrow[2] and until now the method of isolating bone marrow derived MKs has been complicated and only resulted in limited MKs[129]. Although some studies reported that they can get relatively purified bone marrow derived MKs through flow cytometry sorting or HSCs/HSPCs culturing, they can only harvest a small number of MKs [6][132].

In our method, after percoll purification we aspirated the first 4ml liquids to culture the megakaryocytes. It was important to pay attention to the cell number

that in all 10^7 cells should be added into each well of the 6-well plate. We owe the success of MK culturing model to the effect of cytokines and the support from different lineage cells. TPO has been confirmed to be a potent and particularly well-known megakaryopoiesis activator[133][134]. And evidence has also shown that IL-6 can induce the development of MKs[135][136][137]. IL-6 is normally secreted by macrophages and T cells and it can stimulate the megakaryopoiesis and thrombopoiesis. It has been reported that through secreting IL-9 the osteoblasts can support the megakaryopoiesis[138]. Kenneth Kaushansky similarly found that MKs can arise in colonies that containing one or more lineage cells[139].

Although we successfully stained SDF1 in the isolated MKs, we did not manage to do so in the bone marrow section (Figure 3.34). The major possible cause is that the clone of SDF1 antibody is mouse anti-mouse, which will lead to more unspecific binding to other bone marrow cells and present as a high background. We then introduced the CXCL12-DsRed mice, which the DsRed signal has been labeled on CXCL12 automatically. However, we did not find the DsRed signal at the position where there were MKs. The result suggests us that perhaps SDF1 is expressed at a relatively low level in MKs. Some reports[114][132] and our western blot experiment have proved this.

4.2 Definition of megakaryocyte progenitors and cell isolation protocol

Before we introduced the vWF-eGFP mouse model, we tried to use the wild-type mice to conduct the MK-MKp transwell experiment. However, there would still

be some MKps mixed in the isolated MKs even after two times of BSA gradient. As we would mark all of the cells in the lower chamber (including the migrated MKps and MKps mixed in the MKs) with the CD41 marker, it would be difficult to distinguish the migrated MKps from the original existed MKps. From the study of Alejandra S et al. we know that most MKps in the vWF-eGFP mouse strain will be GFP positive[14]. This considered, along with the research of Simmon Haas et al. [6], we decided to define MKps as Lineage$^-$Scal1$^-$C-kit$^+$vWF-eGFP$^+$ cells in our transmigration experiment.

At the beginning, we tried to perform the megakaryocyte progenitors isolation through flow cytometry sorting technique, however, only 1.1x10^5 events (from 6 mice) could be sorted. But the real number of the live MKps would be far less than expected, because of the fake positive signals, technique errors and dead cells mixed in the sorted cells. At the same time, the long length of the sorting procedure will also hurt the cells. For this reason, we finally decided to use the bone marrow cells that purified after percoll to harvest MKps. We found that normally the MKp fraction were approximately 0.5% (tested by FACs) after the percoll purification. We then put 2x10^6 cells (which contain 10^4 MKps) in the transwell inserts. In this way we were able to get MKps in a more efficient way and with easier handling. As the pressure in and out of the transwell insert should be maintained the same, we ensured that we normally put less than 200ul liquid in an insert. Otherwise, the unbalanced pressure would push more cells to migrate to the lower chamber and lead the experiment to fail.

Although our MKps isolation is a more stable and convenient method than sorting, it has a shortcoming. As there are large amounts of other lineage cells in the $2x10^6$ cells, some cells that can be easily triggered by SDF1 like neutrophils will also migrate through the 5 um pore of the transwell inserts. This must be a competitor to the MKps' chemotaxis migration towards SDF1. Besides this, less CXCR4 expression on the surface of MKps can also explain why MKps cannot migrate potently towards the SDF1 gradient (Figure 3.71).

After the SDF1 trans-migration model was established, we next investigated whether mature MKs can attract the migration of MKps. However, the result showed us that nearly no MKp migrated towards the MKs. Neither the TPO nor the TPO triggered mature MKs had a chemotaxis attraction effect on MKps. Until now, very few studies have reported that other chemokines can trigger the migration of MKps except for SDF1[140]. If so, considering mature MKs can only express a low level of SDF1, it is explicable why mature MKs cannot trigger the migration of MKps.

4.3 CXCR7-CXCL12 and AMD 3100

As it is mentioned in the introduction section, CXCR4 is not the only one receptor of CXCL12, which CXCL12-CXCR7 has been proved to direct lymphoid T cells migration independent from CXCR4[105]. CXCR7 is reported to be expressed on neutrophils, monocytes, and B-cells[104][107][141]. Frederic Sierro et al. proved that CXCR7 is crucial to the proliferation and differentiation of endothelial cells[139]. This receptor is also essential in the cell survival and

adhesion[105]. Mice of CXCR7 knockout cannot survive due to the ontogeny dysfunction [107][108]. As a competitor binding ligand, the CXCL12-CXCR7 binding has been proved to reduce the CXCL12-CXCR4 binding[142]. As it is shown in Figure 1.1.4.1, CXCR7 can act as a mediator in CXCL12-induced MAPK activation independently from CXCR4[143]. Except this, CXCR7 can compound with CXCR4 as a heterodimer and activate the β-arrestin-mediated signaling together to induce cell migration[144] (Figure 1.1.4.1). In which they found that the CXCR7-CXCL12 chemotaxis effect is independent from CXCR4 through the using of AMD 3100.

AMD 3100 (also known as plexifor) is a well-known CXCR4 antagonist. Previous studies presented that AMD 3100 can cooperate with C-GSF in the treatment of multiple myeloma and blood diseases such as non-Hodgkin's lymphoma[98]. Although CXCR4 is a co-receptor to the HIV surface glycoprotein and FDA has approved AMD 3100 to be a HIV drug therapy, its side effects such as cardiovascular toxicity continue to make this therapy controversial [145].

AMD3100 prevents the binding of CXCL12 to CXCR4, thus blocking the CXCR4-induced intracellular signaling (Figure 1.1.4.1). Considering this, AMD3100 has also been proved to be an indirect trigger for CXCR7, which can increase the CXCL12 binding to CXCR7[146]. This research about CXCL12-CXCR7 axis makes it even more complicated for all of the studies focusing on the CXCL12-CXCR4 axis.

4.4 AMD 3100 in vitro experiment results

In our in vitro trans-migration experiment, fewer MKps could migrate towards the SDF1 gradient when the cells were pre-incubated with AMD 3100. Combined with the positive effect of SDF1 chemotaxis to MKps, this showed us that CXCL12-CXCR4 axis triggered MKps migration towards the SDF1 gradient.

According to some reports, CXCR4 and CXCR7 can be expressed at different levels on different cells[147][148][149][150]. Until now there has been no report about the expression of CXCR7 on hematopoietic cells. As both of the two receptors can combine with CXCL12 and trigger the chemo-attraction, the effect will be decided by the expression of CXCR4 and CXCR7 on the cell surface. According to D Rath et al. platelets can express both CXCR4 and CXCR7[151]. In this way, the result of our in vitro trans-migration experiment may indicate to us that the CXCR7 expression on MKps may be at a weak level and similar results have also been reported by R. Maksym[152]. Compared to CXCR7, CXCR4 will be the main receptor to CXCL12 on the surface of MKps.

4.5 AMD 3100 in vivo experiment results

In our in vivo experiment, we firstly treated the mice with AMD 3100 in sequential 5 days in a dose of 1mg/kg/day. A trend arose that MKs and MKps changed their positions in the bone marrow and moved away from the vessels after the interference of AMD 3100 (figure 3.82 A and C). However, we did not observe significant platelet decrease (figure 3.81 A). Similar results have been reported[85] that the circulating platelets slightly decreased 1h after AMD 3100 injection, however, after 24h the platelets recovered to a normal level. This may

explain why we did not observe significant change of the peripheral platelets after 5 days AMD 3100 treatment, as our blood measurement time point is every 24 hours.

Previous studies reported that AMD3100 can prevent neutrophils from going back to the bone marrow niche and the blood neutrophils peaks will be in 1-2.5 hours after AMD3100 treatment[153][154]. That may be why in our experiment we did not manage to observe the up-regulation of circulating neutrophils after AMD 3100 treatment (figure 3.81 B). The main reason is that our blood measurement time point is every 24 hours after AMD 3100 treatment instead of 1-2.5 hours. According to the study of Hendrix et al., WBC counts will reach a blood concentration peak 0.25-1.2 hours after treating with different dose of AMD 3100 and return to baseline after 24 hours[155]. The plasma half-life of the drug is very short only 3-5 hours and within 24 hours 70% of the drug will be excreted [156].

There is no obvious change in MK and MKps numbers in both of the two groups (Fig 3.8.2). For the MKs, most of the MKs attach to the vessels at stable state. (1) According to the in vitro CXCL12-CXCR4 experiment from D. Stegner et al. [85], there is no need for MKs to migrate to vessel due to the high density of sinusoids vessels. This may also explain why MKs only migrate slightly away from the vessels when treated by AMD 3100. In parallel to this, the platelet level remains stable after 24h of AMD3100 treatment. Even when there may be a fluctuation of MKs attached to the vessels, MKps can replenish the MKs directly as most of the

MKps also attach to the vessels. (2) The study conducted by David. S et al. also found that the number of MKs and platelets will not change obviously after 24 hours of AMD 3100 treatment[85]. If there is no stress on both platelets and MKs, it is understandable that the number of MKps remains unchanged after AMD 3100 treatment. (3) Due to the low level expression of CXCR4 on MKps and the transient drug effect of AMD3100, the drug may not affect the movement of MKps significantly. This has been shown in our in vitro experiment. It may be why we did not observe significant change of cell position after 24h of AMD 3100 treatment. (4) Although some MKs and MKps slightly changed their position away from the vessels after 5 days AMD 3100 treatment, there were still large amounts of MKs and MKps attached to the vessels, which can maintain the homeostasis of thrombopoiesis and megakaryopoiesis.

Except for investigating the effect of AMD 3100 at steady state, we next examined how AMD3100 interferes platelet recovering in the mice treated with platelet depletion. The neutrophils in combination group (AMD 3100 and platelet depletion group) did not show an up-regulating trend compared to platelet depletion (PD) group (Figure 3.8.3 B). The main reason may be the same as the explanation we provided in AMD 3100 treatment experiment at steady state. The platelet recovering in combination group has no statistical significance compared with that in PD group (Figure 3.8.3 A). Whole-mount staining analysis showed us that the position of most MKs and MKps remained attached to the vessels in both of the two groups (Figure 3.8.4 A and C) and the cell numbers had

no statistical significance in each cell-vessel distance range. The number of MKs and MKps did not change obviously (Figure 3.8.4 B and D).

The MK numbers will remain stable after the platelet depletion (Figure 1.1.3.6). As we previously explained, MKps can differentiate into MKs to replenish the loss of differentiated MKs. Most of the MKs have already attached to the vessels and due to the low vessel-to vessel distance, MKs can easily reach the vessels even when the CXCR4 is blocked[85]. So the reason why the position and number of MKs did not change obviously in combination group should be the reason why that did not change significantly in AMD 3100 treatment group at steady state.

Large amounts of MKps will differentiate into MKs after platelet depletion, which is mainly induced by TPO. Different from the stability of MK numbers, MKps up-regulated obviously after platelet depletion. Some studies proved that SDF1 can trigger the proliferation and maturation of MKps only when TPO existed [77][119]. At the same time, our preliminary TPO-Elisa test showed us that the TPO level under the platelet depletion stimuli is obviously up-regulated (Figure 1.1.3.12)[Dissertation, Wenwen Fu, LMU, 2017]. In parallel, our Edu FACs experiment testified that platelet depletion can trigger the proliferation of MKps (Figure 1.1.3.13)[Dissertation, Wenwen Fu, LMU, 2017].

From our chemokine kit data we know that SDF1 remains a high level in the bone marrow not only at stable state but also in the mice treated with platelet depletion (Figure 3.3.7). The CXCL12 abundant reticular (CAR) cells can express

extremely high level of CXCL12[115]. Meanwhile, these cells locate in the endothelial cell niche[157]where there are large amounts of MKs and MKps [114]. Based on these researches, we can hypothesize that MKps proliferation should be inhibited when CXCR4 is blocked. However, in our in vivo data we did not observe a significant decrease of MKps.

There are several possible reasons for this: (1) Due to the lower expression of CXCR4 on the surface of MKps, the AMD 3100 cannot affect the migration of MKps significantly. And most of the MKps reside close to the vessels, like MKs, can easily reach the vessels due to the high density of sinusoids vessels. (2) Similarly, as we illustrated before, AMD 3100 performed the CXCR4 blocking effect for only a short period. (3) Thirdly, it is reported that CXCR7 expression will be up-regulated after AMD3100 treatment and CXCL12 can better combine to CXCR7[146]. Although the CXCR7-CXCL12 axis may not play a main role in the MKps migration, it may activate the other bone marrow linage cells like endothelial cells, neutrophils, lymphocytes that may affect the megakaryopoiesis. And different kinds of cells, cytokines and chemokines orchestrate a complicated system, which makes it more difficult for us to uncover their effect on megakaryopoiesis by focusing on only one or two ligand/receptor modulation in situ.

Combined with that SDF1 has not only one receptor and the study on CXCL12/CXCR7 remains unclear, the reason why we did not observe an obvious effect of AMD 3100 on the location and numbers of MKs and MKps at steady

state or under platelet depletion stimuli may due to the complex interaction of cells and cytokines in the bone marrow microenvironment, as well as the drug half life.

Except for this, the AMD3100 treatment experiment has another shortcoming. The AMD3100 is a global CXCR4 antagonist, which means that all the CXCR4 will be blocked in situ. This will complicate the in vivo analysis of the direct effect of CXCL12-CXCR4 axis on the megakaryopoiesis.

Above all, the work of this thesis was able to successfully culture the bone marrow derived megakaryocytes in a large amount within a short time. This paved the way for better studies on bone marrow derived MKs. Moreover, the transmigration model can not only benefit our SDF1, MK-MKp chemotaxis experiment but also enable us to test the effect of other cytokines or chemokines on MKps.

5. References

[1] K. R. Machlus and J. E. Italiano, "The incredible journey: From megakaryocyte development to platelet formation," *J. Cell Biol.*, vol. 201, no. 6, pp. 785–796, 2013.

[2] J. L. Richardson, R. A. Shivdasani, C. Boers, J. H. Hartwig, and J. E. Italiano, "Mechanisms of organelle transport and capture along proplatelets during platelet production," *Blood*, vol. 106, no. 13, pp. 4066–4075, 2005.

[3] M. W. Long, N. Williams, and S. Ebbe, "Immature megakaryocytes in the mouse: physical characteristics, cell cycle status, and in vitro responsiveness to thrombopoietic stimulatory factor.," *Blood*, vol. 59, no. 3, pp. 569–75, 1982.

[4] M. Ogawa, "Differentiation and proliferation of hematopoietic stem cells.," *Blood*, vol. 81, no. 11, pp. 2844–53, 1993.

[5] Y. Morita, A. Iseki, S. Okamura, S. Suzuki, H. Nakauchi, and H. Ema, "Functional characterization of hematopoietic stem cells in the spleen," *Exp. Hematol.*, vol. 39, no. 3, 2011.

[6] S. Haas, J. Hansson, D. Klimmeck, D. Loeffler, L. Velten, H. Uckelmann, S. Wurzer, Á. M. Prendergast, A. Schnell, K. Hexel, R. Santarella-Mellwig, S. Blaszkiewicz, A. Kuck, H. Geiger, M. D. Milsom, L. M. Steinmetz, T. Schroeder, A. Trumpp, J. Krijgsveld, and M. A. G. Essers, "Inflammation-Induced Emergency Megakaryopoiesis Driven by Hematopoietic Stem Cell-like Megakaryocyte Progenitors," *Cell Stem Cell*, vol. 17, no. 4, pp. 422–434, 2015.

[7] S. J. Morrison, a M. Wandycz, H. D. Hemmati, D. E. Wright, and I. L. Weissman, "Identification of a lineage of multipotent hematopoietic progenitors.," *Development*, vol. 124, no. 10, pp. 1929–39, 1997.

[8] K. Akashi, D. Traver, T. Miyamoto, and I. L. Weissman, "A clonogenic common myeloid progenitor that gives rise to all myeloid lineages," *Nature*, vol. 404, no. 6774, pp. 193–197, 2000.

[9] M. Kondo, I. L. Weissman, and K. Akashi, "Identification of Clonogenic Common Lymphoid Progenitors in Mouse Bone Marrow," *Cell*, vol. 91, no. 5, pp. 661–672, 1997.

[10] N. Debili, L. Coulombel, L. Croisille, A. Katz, J. Guichard, J. Breton-Gorius, and W. Vainchenker, “Characterization of a bipotent erythro-megakaryocytic progenitor in human bone marrow.,” *Blood*, vol. 88, no. 4, pp. 1284–1296, 1996.

[11] L. Pang, M. J. Weiss, and M. Poncz, “Megakaryocyte biology and related disorders,” *Journal of Clinical Investigation*, vol. 115, no. 12. pp. 3332–3338, 2005.

[12] J. Adolfsson, R. Månsson, N. Buza-Vidas, A. Hultquist, K. Liuba, C. T. Jensen, D. Bryder, L. Yang, O.-J. Borge, L. A. M. Thoren, K. Anderson, E. Sitnicka, Y. Sasaki, M. Sigvardsson, and S. E. W. Jacobsen, “Identification of Flt3+ Lympho-Myeloid Stem Cells Lacking Erythro-Megakaryocytic Potential,” *Cell*, vol. 121, no. 2, pp. 295–306, 2005.

[13] E. C. Forsberg, T. Serwold, S. Kogan, I. L. Weissman, E. Passegué, J. Adolfsson, O. J. Borge, D. Bryder, K. Theilgaard-Monch, I. Astrand-Grundstrom, E. Sitnicka, Y. Sasaki, S. E. Jacobsen, J. Adolfsson, R. Mansson, N. Buza-Vidas, A. Hultquist, K. Liuba, C. T. Jensen, D. Bryder, L. Yang, O. J. Borge, L. A. Thoren, et al., K. Akashi, D. Traver, T. Miyamoto, I. L. Weissman, K. Akashi, D. Traver, L. I. Zon, Y. A. Cao, A. J. Wagers, A. Beilhack, J. Dusich, M. H. Bachmann, R. S. Negrin, I. L. Weissman, C. H. Contag, J. L. Christensen, I. L. Weissman, A. Cumano, I. Godin, A. D’Amico, L. Wu, E. C. Forsberg, S. S. Prohaska, S. Katzman, G. C. Heffner, J. M. Stuart, I. L. Weissman, M. A. Goodell, K. Brose, G. Paradis, A. S. Conner, R. C. Mulligan, H. Hock, S. H. Orkin, K. Ikuta, I. L. Weissman, K. Ikuta, T. Kina, I. MacNeil, N. Uchida, B. Peault, Y. H. Chien, I. L. Weissman, N. B. Ivanova, J. T. Dimos, C. Schaniel, J. A. Hackney, K. A. Moore, I. R. Lemischka, M. J. Kiel, O. H. Yilmaz, T. Iwashita, O. H. Yilmaz, C. Terhorst, S. J. Morrison, A. G. King, M. Kondo, D. C. Scherer, I. L. Weissman, M. Kondo, I. L. Weissman, K. Akashi, M. Kondo, D. C. Scherer, T. Miyamoto, A. G. King, K. Akashi, K. Sugamura, I. L. Weissman, A. Y. Lai, S. M. Lin, M. Kondo, K. Mackarehtschian, J. D. Hardin, K. A. Moore, S. Boast, S. P. Goff, I. R. Lemischka, T. Miyamoto, H. Iwasaki, B. Reizis, M. Ye, T. Graf, I. L. Weissman, K. Akashi, S. J. Morrison, I. L. Weissman, S. J. Morrison, D. E. Wright, I. L. Weissman, T. N. Nakorn, D. Traver, I. L. Weissman, K. Akashi, T. N. Nakorn, T. Miyamoto, I. L. Weissman, S. L. Nutt,

B. Heavey, A. G. Rolink, M. Busslinger, S. L. Nutt, D. Metcalf, A. D'Amico, M. Polli, L. Wu, M. Osawa, K. Hanada, H. Hamada, H. Nakauchi, E. Passegué, A. J. Wagers, S. Guiriato, W. Anderson, I. L. Weissman, D. J. Rossi, D. Bryder, J. M. Zahn, H. Ahlenius, R. Sonu, A. J. Wagers, I. L. Weissman, L. G. Smith, I. L. Weissman, S. Heimfeld, M. Socolovsky, H. Nam, M. D. Fleming, V. H. Haase, C. Brugnara, H. F. Lodish, G. J. Spangrude, S. Heimfeld, I. L. Weissman, H. Takano, H. Ema, K. Sudo, H. Nakauchi, A. V. Terskikh, T. Miyamoto, C. Chang, L. Diatchenko, I. L. Weissman, A. J. Wagers, R. I. Sherwood, J. L. Christensen, I. L. Weissman, I. L. Weissman, D. E. Wright, S. H. Cheshier, A. J. Wagers, T. D. Randall, J. L. Christensen, I. L. Weissman, H. Xie, M. Ye, R. Feng, T. Graf, L. Yang, D. Bryder, J. Adolfsson, J. Nygren, R. Mansson, M. Sigvardsson, and S. E. Jacobsen, "New evidence supporting megakaryocyte-erythrocyte potential of flk2/flt3+ multipotent hematopoietic progenitors.," *Cell*, vol. 126, no. 2, pp. 415–26, 2006.

[14] A. Sanjuan-Pla, I. C. Macaulay, C. T. Jensen, P. S. Woll, T. C. Luis, A. Mead, S. Moore, C. Carella, S. Matsuoka, T. B. Jones, O. Chowdhury, L. Stenson, M. Lutteropp, J. C. A. Green, R. Facchini, H. Boukarabila, A. Grover, A. Gambardella, S. Thongjuea, J. Carrelha, P. Tarrant, D. Atkinson, S. A. Clark, C. Nerlov, and S. E. W. Jacobsen, "Platelet-biased stem cells reside at the apex of the haematopoietic stem-cell hierarchy," *Nature*, vol. 502, no. 7470, pp. 232–236, 2013.

[15] M. A. Stark, Y. Huo, T. L. Burcin, M. A. Morris, T. S. Olson, and K. Ley, "Phagocytosis of apoptotic neutrophils regulates granulopoiesis via IL-23 and IL-17," *Immunity*, vol. 22, no. 3, pp. 285–294, 2005.

[16] S. Bugl, S. Wirths, M. P. Radsak, H. Schild, P. Stein, M. C. André, M. R. Müller, E. Malenke, T. Wiesner, M. Märklin, J. S. Frick, R. Handgretinger, H. G. Rammensee, L. Kanz, and H. G. Kopp, "Steady-state neutrophil homeostasis is dependent on TLR4/TRIF signaling," *Blood*, vol. 121, no. 5, pp. 723–733, 2013.

[17] P. O. Scumpia, K. M. Kelly-Scumpia, M. J. Delano, J. S. Weinstein, A. G. Cuenca, S. Al-Quran, I. Bovio, S. Akira, Y. Kumagai, and L. L. Moldawer, "Cutting edge: bacterial infection induces hematopoietic stem and progenitor cell expansion in the absence of TLR signaling.," *J. Immunol.*, vol.

184, no. 5, pp. 2247–2251, 2010.

[18] M. a G. Essers, S. Offner, W. E. Blanco-Bose, Z. Waibler, U. Kalinke, M. a Duchosal, and A. Trumpp, "IFNalpha activates dormant haematopoietic stem cells in vivo.," *Nature*, vol. 458, no. 7240, pp. 904–8, 2009.

[19] N. Mossadegh-Keller, S. Sarrazin, P. K. Kandalla, L. Espinosa, E. Richard Stanley, S. L. Nutt, J. Moore, and M. H. Sieweke, "M-CSF instructs myeloid lineage fate in single haematopoietic stem cells," *Nature*, vol. 497, no. 7448, pp. 239–243, 2013.

[20] A. Ehninger, T. Boch, H. Uckelmann, M. a Essers, K. Müdder, B. P. Sleckman, and A. Trumpp, "Post-transcriptional regulation of c-Myc expression in adult murine HSCs during homeostasis and interferon-α induced stress response.," *Blood*, vol. 123, no. 25, pp. 3909–3913, 2014.

[21] N. Cabezas-Wallscheid, D. Klimmeck, J. Hansson, D. B. Lipka, A. Reyes, Q. Wang, D. Weichenhan, A. Lier, L. Von Paleske, S. Renders, P. Wünsche, P. Zeisberger, D. Brocks, L. Gu, C. Herrmann, S. Haas, M. A. G. Essers, B. Brors, R. Eils, W. Huber, M. D. Milsom, C. Plass, J. Krijgsveld, and A. Trumpp, "Identification of regulatory networks in HSCs and their immediate progeny via integrated proteome, transcriptome, and DNA methylome analysis," *Cell Stem Cell*, vol. 15, no. 4, pp. 507–522, 2014.

[22] J. Zimmet and K. Ravid, "Polyploidy: Occurrence in nature, mechanisms, and significance for the megakaryocyte-platelet system," *Experimental Hematology*, vol. 28, no. 1. pp. 3–16, 2000.

[23] K. Ravid, J. Lu, J. M. Zimmet, and M. R. Jones, "Roads to polyploidy: The megakaryocyte example," *Journal of Cellular Physiology*, vol. 190, no. 1. pp. 7–20, 2002.

[24] G. Mattia, F. Vulcano, L. Milazzo, A. Barca, G. Macioce, A. Giampaolo, and H. Jane Hassan, "Different ploidy levels of megakaryocytes generated from peripheral or cord blood CD34+ cells are correlated with different levels of platelet release," *Blood*, vol. 99, no. 3, pp. 888–897, 2002.

[25] R. Miyazaki, H. Ogata, T. Iguchi, S. Sogo, T. Kushida, T. Ito, M. Inaba, S. Ikehara, and Y. Kobayashi, "Comparative analyses of megakaryocytes derived from cord blood and bone marrow," *Br J Haematol*, vol. 108, no. 3, pp. 602–609, 2000.

[26] H. Raslova, A. Kauffmann, D. Sekkaï, H. Ripoche, F. Larbret, T. Robert, D. T. Le Roux, G. Kroemer, N. Debili, P. Dessen, V. Lazar, and W. Vainchenker, "Interrelation between polyploidization and megakaryocyte differentiation: A gene profiling approach," *Blood*, vol. 109, no. 8, pp. 3225–3234, 2007.

[27] D. Bluteau, L. Lordier, A. Di Stefano, Y. Chang, H. Raslova, N. Debili, and W. Vainchenker, "Regulation of megakaryocyte maturation and platelet formation," *Journal of Thrombosis and Haemostasis*, vol. 7, no. SUPPL. 1. pp. 227–234, 2009.

[28] Z. J. Liu, J. Italiano, F. Ferrer-Marin, R. Gutti, M. Bailey, B. Poterjoy, L. Rimsza, and M. Sola-Visner, "Developmental differences in megakaryocytopoiesis are associated with up-regulated TPO signaling through mTOR and elevated GATA-1 levels in neonatal megakaryocytes," *Blood*, vol. 117, no. 15, pp. 4106–4117, 2011.

[29] E. Hegyi, S. Navarro, N. Debili, M. -A Mouthon, A. Katz, J. Breton-Gorius, and W. Vainchenker, "Regulation of human megakaryocytopoiesis: Analysis of proliferation, ploidy and maturation in liquid cultures," *Int. J. Cell Cloning*, vol. 8, no. 4, pp. 236–244, 1990.

[30] Y. X. Ru, S. X. Zhao, S. X. Dong, Y. Q. Yang, and B. Eyden, "On the Maturation of Megakaryocytes: A Review with Original Observations on Human in Vivo Cells Emphasizing Morphology and Ultrastructure," *Ultrastructural Pathology*, vol. 39, no. 2. pp. 79–87, 2015.

[31] K. Miyawaki, H. Iwasaki, T. Jiromaru, H. Kusumoto, A. Yurino, T. Sugio, Y. Uehara, J. Odawara, S. Daitoku, Y. Kunisaki, Y. Mori, Y. Arinobu, H. Tsuzuki, Y. Kikushige, T. Iino, K. Kato, K. Takenaka, T. Miyamoto, T. Maeda, and K. Akashi, "Identification of unipotent megakaryocyte progenitors in human hematopoiesis," *Blood*, vol. 129, no. 25, pp. 3332–3343, 2017.

[32] R. F. Levine, K. C. Hazzard, and J. D. Lamberg, "The significance of megakaryocyte size.," *Blood*, vol. 60, no. 5, pp. 1122–31, 1982.

[33] C. E. Carow, N. E. Fox, and K. Kaushansky, "Kinetics of endomitosis in primary murine megakaryocytes," *J. Cell. Physiol.*, vol. 188, no. 3, pp. 291–303, 2001.

[34] J. N. Thon, A. Montalvo, S. Patel-Hett, M. T. Devine, J. L. Richardson, A.

Ehrlicher, M. K. Larson, K. Hoffmeister, J. H. Hartwig, and J. E. Italiano, "Cytoskeletal mechanics of proplatelet maturation and platelet release," *J. Cell Biol.*, vol. 191, no. 4, pp. 861–874, 2010.

[35] E. S. Choi, J. L. Nichol, M. M. Hokom, A. C. Hornkohl, and P. Hunt, "Platelets generated in vitro from proplatelet-displaying human megakaryocytes are functional.," *Blood*, vol. 85, no. 2, pp. 402–413, 1995.

[36] N. Debili, C. Robin, V. Schiavon, R. Letestu, F. Pflumio, M. T. Mitjavila-Garcia, L. Coulombel, and W. Vainchenker, "Different expression of CD41 on human lymphoid and myeloid progenitors from adults and neonates," *Blood*, vol. 97, no. 7, pp. 2023–2030, 2001.

[37] A. Sanjuan-Pla, I. C. Macaulay, C. T. Jensen, P. S. Woll, T. C. Luis, A. Mead, S. Moore, C. Carella, S. Matsuoka, T. B. Jones, O. Chowdhury, L. Stenson, M. Lutteropp, J. C. Green, R. Facchini, H. Boukarabila, A. Grover, A. Gambardella, S. Thongjuea, J. Carrelha, P. Tarrant, D. Atkinson, S. A. Clark, C. Nerlov, and S. E. Jacobsen, "Platelet-biased stem cells reside at the apex of the haematopoietic stem-cell hierarchy," *Nature*, vol. 502, no. 7470, pp. 232–236, 2013.

[38] J. Y. Shin, W. Hu, M. Naramura, and C. Y. Park, "High c-Kit expression identifies hematopoietic stem cells with impaired self-renewal and megakaryocytic bias," *J. Exp. Med.*, vol. 211, no. 2, pp. 217–231, 2014.

[39] O. Klimchenko, M. Mori, A. DiStefano, T. Langlois, F. Larbret, Y. Lecluse, O. Feraud, W. Vainchenker, F. Norol, and N. Debili, "A common bipotent progenitor generates the erythroid and megakaryocyte lineages in embryonic stem cell-derived primitive hematopoiesis," *Blood*, vol. 114, no. 8, pp. 1506–1517, 2009.

[40] A. H. Lagrue-Lak-Hal, N. Debili, G. Kingbury, C. Lecut, J. P. Le Couedic, J. L. Villeval, M. Jandrot-Perrus, and W. Vainchenker, "Expression and Function of the Collagen Receptor GPVI during Megakaryocyte Maturation," *J. Biol. Chem.*, vol. 276, no. 18, pp. 15316–15325, 2001.

[41] Y. Chang, D. Bluteau, N. Debili, and W. Vainchenker, "From hematopoietic stem cells to platelets," *J Thromb Haemost*, vol. 5 Suppl 1, pp. 318–327, 2007.

[42] G. Szalai, A. C. LaRue, and D. K. Watson, "Molecular mechanisms of

megakaryopoiesis," *Cellular and Molecular Life Sciences*, vol. 63, no. 21. pp. 2460–2476, 2006.

[43] R. A. Shivdasani, Y. Fujiwara, M. A. McDevitt, and S. H. Orkin, "A lineage-selective knockout establishes the critical role of transcription factor GATA-1 in megakaryocyte growth and platelet development," *EMBO J.*, vol. 16, no. 13, pp. 3965–3973, 1997.

[44] P. Vyas, K. Ault, C. W. Jackson, S. H. Orkin, and R. a Shivdasani, "Consequences of GATA-1 deficiency in megakaryocytes and platelets," *Blood*, vol. 93, no. 9, pp. 2867–2875, 1999.

[45] A. M. Vannucchi, L. Bianchi, C. Cellai, F. Paoletti, R. A. Rana, R. Lorenzini, G. Migliaccio, and A. R. Migliaccio, "Development of myelofibrosis in mice genetically impaired for GATA-1 expression (GATA-1low mice)," *Blood*, vol. 100, no. 4, pp. 1123–1132, 2002.

[46] A. P. Tsang, Y. Fujiwara, D. B. Horn, and S. H. Orkin, "Failure of megakaryopoiesis and arrested erythropoiesis in mice lacking the GATA-1 transcriptional cofactor FOG," *Genes Dev.*, vol. 12, no. 8, pp. 1176–1188, 1998.

[47] M. Ichikawa, T. Asai, T. Saito, G. Yamamoto, S. Seo, I. Yamazaki, T. Yamagata, K. Mitani, S. Chiba, H. Hirai, S. Ogawa, and M. Kurokawa, "AML-1 is required for megakaryocytic maturation and lymphocytic differentiation, but not for maintenance of hematopoietic stem cells in adult hematopoiesis," *Nat. Med.*, vol. 10, no. 3, pp. 299–304, 2004.

[48] J. E. Draper, P. Sroczynska, H. S. Leong, M. Z. H. Fadlullah, C. Miller, V. Kouskoff, and G. Lacaud, "Mouse RUNX1C regulates premegakaryocytic/erythroid output and maintains survival of megakaryocyte progenitors," *Blood*, vol. 130, no. 3, pp. 271–284, 2017.

[49] O. N. Kuvardina, J. Herglotz, S. Kolodziej, N. Kohrs, S. Herkt, B. Wojcik, T. Oellerich, J. Corso, K. Behrens, A. Kumar, H. Hussong, H. Urlaub, J. Koch, H. Serve, H. Bonig, C. Stocking, M. A. Rieger, and J. Lausen, "RUNX1 represses the erythroid gene expression program during megakaryocytic differentiation," *Blood*, vol. 125, no. 23, pp. 3570–3579, 2015.

[50] S. Saleque, S. Cameron, and S. H. Orkin, "The zinc-finger proto-oncogene Gfi-1b is essential for development of the erythroid and megakaryocytic

lineages," *Genes Dev.*, vol. 16, no. 3, pp. 301–306, 2002.

[51] Z. Chen, M. Hu, and R. A. Shivdasani, "Expression analysis of primary mouse megakaryocyte differentiation and its application in identifying stage-specific molecular markers and a novel transcriptional target of NF-E2," *Blood*, vol. 109, no. 4, pp. 1451–1459, 2007.

[52] R. A. Shivdasani, M. F. Rosenblatt, D. Zucker-Franklin, C. W. Jackson, P. Hunt, C. J. M. Saris, and S. H. Orkin, "Transcription factor NF-E2 is required for platelet formation independent of the actions of thrombopoeitin/MGDF in megakaryocyte development," *Cell*, vol. 81, no. 5, pp. 695–704, 1995.

[53] N. Emambokus, A. Vegiopoulos, B. Harman, E. Jenkinson, G. Anderson, and J. Frampton, "Progression through key stages of haemopoiesis is dependent on distinct threshold levels of c-Myb," *EMBO J.*, vol. 22, no. 17, pp. 4478–4488, 2003.

[54] M. R. Carpinelli, D. J. Hilton, D. Metcalf, J. L. Antonchuk, C. D. Hyland, S. L. Mifsud, L. Di Rago, A. A. Hilton, T. A. Willson, A. W. Roberts, R. G. Ramsay, N. A. Nicola, and W. S. Alexander, "From The Cover: Suppressor screen in Mpl-/- mice: c-Myb mutation causes supraphysiological production of platelets in the absence of thrombopoietin signaling," *Proc. Natl. Acad. Sci.*, vol. 101, no. 17, pp. 6553–6558, 2004.

[55] A. Hart, F. Melet, P. Grossfeld, K. Chien, C. Jones, A. Tunnacliffe, R. Favier, and A. Bernstein, "Fli-1 is required for murine vascular and megakaryocytic development and is hemizygously deleted in patients with thrombocytopenia," *Immunity*, vol. 13, no. 2, pp. 167–177, 2000.

[56] L. Pang, H. H. Xue, G. Szalai, X. Wang, Y. Wang, D. K. Watson, W. J. Leonard, G. A. Blobel, and M. Poncz, "Maturation stage-specific regulation of megakaryopoiesis by pointed-domain Ets proteins," *Blood*, vol. 108, no. 7, pp. 2198–2206, 2006.

[57] V. Lulli, P. Romania, O. Morsilli, M. Gabbianelli, A. Pagliuca, S. Mazzeo, U. Testa, C. Peschle, and G. Marziali, "Overexpression of Ets-1 in human hematopoietic progenitor cells blocks erythroid and promotes megakaryocytic differentiation," *Cell Death Differ.*, vol. 13, no. 7, pp. 1064–1074, 2006.

[58] J. Lu, S. Guo, B. L. Ebert, H. Zhang, X. Peng, J. Bosco, J. Pretz, R. Schlanger, J. Y. Wang, R. H. Mak, D. M. Dombkowski, F. I. Preffer, D. T. Scadden, and T. R. Golub, "MicroRNA-Mediated Control of Cell Fate in Megakaryocyte-Erythrocyte Progenitors," *Dev. Cell*, vol. 14, no. 6, pp. 843–853, 2008.

[59] C. Labbaye, I. Spinello, M. T. Quaranta, E. Pelosi, L. Pasquini, E. Petrucci, M. Biffoni, E. R. Nuzzolo, M. Billi, R. Foà, E. Brunetti, F. Grignani, U. Testa, and C. Peschle, "A three-step pathway comprising PLZF/miR-146a/CXCR4 controls megakaryopoiesis," *Nat. Cell Biol.*, vol. 10, no. 7, pp. 788–801, 2008.

[60] K. Kaushansky, "Review series The molecular mechanisms that control thrombopoiesis," *J. Clin. Invest.*, vol. 115, no. 12, pp. 3339–3347, 2005.

[61] S. Nishimura, M. Nagasaki, S. Kunishima, A. Sawaguchi, A. Sakata, H. Sakaguchi, T. Ohmori, I. Manabe, J. E. Italiano, T. Ryu, N. Takayama, I. Komuro, T. Kadowaki, K. Eto, and R. Nagai, "IL-1α induces thrombopoiesis through megakaryocyte rupture in response to acute platelet needs," *J. Cell Biol.*, vol. 209, no. 3, pp. 453–466, 2015.

[62] A. P. Ng, M. Kauppi, D. Metcalf, C. D. Hyland, E. C. Josefsson, M. Lebois, J.-G. Zhang, T. M. Baldwin, L. Di Rago, D. J. Hilton, and W. S. Alexander, "Mpl expression on megakaryocytes and platelets is dispensable for thrombopoiesis but essential to prevent myeloproliferation," *Proc. Natl. Acad. Sci.*, vol. 111, no. 16, pp. 5884–5889, 2014.

[63] J. E. Italiano, P. Lecine, R. A. Shivdasani, and J. H. Hartwig, "Blood platelets are assembled principally at the ends of proplatelet processes produced by differentiated megakaryocytes," *J. Cell Biol.*, vol. 147, no. 6, pp. 1299–1312, 1999.

[64] S. R. Patel, J. H. Hartwig, and J. E. Italiano, "The biogenesis of platelets from megakaryocyte proplatelets," *Journal of Clinical Investigation*, vol. 115, no. 12. pp. 3348–3354, 2005.

[65] T. Junt, H. Schulze, Z. Chen, S. Massberg, T. Goerge, A. Krueger, D. D. Wagner, T. Graf, J. E. Italiano, R. A. Shivdasani, and U. H. Von Andrian, "Dynamic visualization of thrombopoiesis within bone marrow," *Science (80-.).*, vol. 317, no. 5845, pp. 1767–1770, 2007.

[66] L. Zhang, M. Orban, M. Lorenz, V. Barocke, D. Braun, N. Urtz, C. Schulz, M.-L. von Brühl, A. Tirniceriu, F. Gaertner, R. L. Proia, T. Graf, S.-S. Bolz, E. Montanez, M. Prinz, A. Müller, L. von Baumgarten, A. Billich, M. Sixt, R. Fässler, U. H. von Andrian, T. Junt, and S. Massberg, "A novel role of sphingosine 1-phosphate receptor S1pr1 in mouse thrombopoiesis," *J. Exp. Med.*, vol. 209, no. 12, pp. 2165–2181, 2012.

[67] J. N. Thon, M. T. Devine, A. J. Begonja, J. Tibbitts, and J. E. Italiano, "High-content live-cell imaging assay used to establish mechanism of trastuzumab emtansine (T-DM1)-mediated inhibition of platelet production," *Blood*, vol. 120, no. 10, pp. 1975–1984, 2012.

[68] Y. Chang, F. Auradé, F. Larbret, Y. Zhang, J. P. Le Couedic, L. Momeux, J. Larghero, J. Bertoglio, F. Louache, E. Cramer, W. Vainchenker, and N. Debili, "Proplatelet formation is regulated by the Rho/ROCK pathway," *Blood*, vol. 109, no. 10, pp. 4229–4236, 2007.

[69] C. Dunois-Lardé, C. Capron, S. Fichelson, T. Bauer, E. Cramer-Bordé, and D. Baruch, "Exposure of human megakaryocytes to high shear rates accelerates platelet production," *Blood*, vol. 114, no. 9, pp. 1875–1883, 2009.

[70] P. Lecine, J. E. Italiano, S. W. Kim, J. L. Villeval, and R. A. Shivdasani, "Hematopoietic-specific beta 1 tubulin participates in a pathway of platelet biogenesis dependent on the transcription factor NF-E2.," *Blood*, vol. 96, no. 4, pp. 1366–73, 2000.

[71] S. R. Patel, J. L. Richardson, H. Schulze, E. Kahle, N. Galjart, K. Drabek, R. A. Shivdasani, J. H. Hartwig, and J. E. Italiano, "Differential roles of microtubule assembly and sliding in proplatelet formation by megakaryocytes," *Blood*, vol. 106, no. 13, pp. 4076–4085, 2005.

[72] H. D. Schwer, P. Lecine, S. Tiwari, J. E. Italiano, J. H. Hartwig, and R. a Shivdasani, "A lineage-restricted and divergent beta-tubulin isoform is essential for the biogenesis, structure and function of blood platelets.," *Curr. Biol.*, vol. 11, no. 8, pp. 579–86, 2001.

[73] S. Kunishima, R. Kobayashi, T. J. Itoh, M. Hamaguchi, and H. Saito, "Mutation of the beta1-tubulin gene associated with congenital macrothrombocytopenia affecting microtubule assembly.," *Blood*, vol. 113,

no. 2, pp. 458–461, 2009.

[74] X. D. Chen, V. Dusevich, J. Q. Feng, S. C. Manolagas, and R. L. Jilka, "Extracellular matrix made by bone marrow cells facilitates expansion of marrow-derived mesenchymal progenitor cells and prevents their differentiation into osteoblasts," *J. Bone Miner. Res.*, vol. 22, no. 12, pp. 1943–1956, 2007.

[75] S. C. Manolagas and R. L. Jilka, "Bone Marrow, Cytokines, and Bone Remodeling — Emerging Insights into the Pathophysiology of Osteoporosis," *N. Engl. J. Med.*, vol. 332, no. 5, pp. 305–311, 1995.

[76] A. A. Ostanin, Y. L. Petrovskii, E. Y. Shevela, and E. R. Chernykh, "Multiplex analysis of cytokines, chemokines, growth factors, MMP-9 and TIMP-1 produced by human bone marrow, adipose tissue, and placental mesenchymal stromal cells," *Bull. Exp. Biol. Med.*, vol. 151, no. 1, pp. 133–141, 2011.

[77] S. T. Avecilla, K. Hattori, B. Heissig, R. Tejada, F. Liao, K. Shido, D. K. Jin, S. Dias, F. Zhang, T. E. Hartman, N. R. Hackett, R. G. Crystal, L. Witte, D. J. Hicklin, P. Bohlen, D. Eaton, D. Lyden, F. De Sauvage, and S. Rafii, "Chemokine-mediated interaction of hematopoietic progenitors with the bone marrow vascular niche is required for thrombopoiesis," *Nat. Med.*, vol. 10, no. 1, pp. 64–71, 2004.

[78] S. C. Pitchford, T. Lodie, and S. M. Rankin, "VEGFR1 stimulates a CXCR4-dependent translocation of megakaryocytes to the vascular niche, enhancing platelet production in mice," in *Blood*, 2012, vol. 120, no. 14, pp. 2787–2795.

[79] M. K. Larson and S. P. Watson, "Regulation of proplatelet formation and platelet release by integrin αIIbβ3," *Blood*, vol. 108, no. 5, pp. 1509–1514, 2006.

[80] S. Sabri, A. Foudi, S. Boukour, B. Franc, S. Charrier, M. Jandrot-Perrus, R. W. Farndale, A. Jalil, M. P. Blundell, E. M. Cramer, F. Louache, N. Debili, A. J. Thrasher, and W. Vainchenker, "Deficiency in the Wiskott-Aldrich protein induces premature proplatelet formation and platelet production in the bone marrow compartment," *Blood*, vol. 108, no. 1, pp. 134–140, 2006.

[81] Z. Zou, A. a Schmaier, L. Cheng, P. Mericko, S. K. Dickeson, T. P. Stricker, S. a

Santoro, and M. L. Kahn, “Negative regulation of activated alpha-2 integrins during thrombopoiesis.,” *Blood*, vol. 113, no. 25, pp. 6428–39, 2009.

[82] I. Pallotta, M. Lovett, W. Rice, D. L. Kaplan, and A. Balduini, “Bone marrow osteoblastic niche: A new model to study physiological regulation of megakaryopoiesis,” *PLoS One*, vol. 4, no. 12, 2009.

[83] H. Schachtner, S. D. J. Calaminus, A. Sinclair, J. Monypenny, M. P. Blundell, C. Leon, T. L. Holyoake, A. J. Thrasher, A. M. Michie, M. Vukovic, C. Gachet, G. E. Jones, S. G. Thomas, S. P. Watson, and L. M. Machesky, “Megakaryocytes assemble podosomes that degrade matrix and protrude through basement membrane,” *Blood*, vol. 121, no. 13, pp. 2542–2552, 2013.

[84] H. Schwertz, S. Köster, W. H. A. Kahr, N. Michetti, B. F. Kraemer, D. A. Weitz, R. C. Blaylock, L. W. Kraiss, A. Greinacher, G. A. Zimmerman, and A. S. Weyrich, “Anucleate platelets generate progeny,” *Blood*, vol. 115, no. 18, pp. 3801–3809, 2010.

[85] D. Stegner, J. M. M. Vaneeuwijk, O. Angay, M. G. Gorelashvili, D. Semeniak, J. Pinnecker, P. Schmithausen, I. Meyer, M. Friedrich, S. Dütting, C. Brede, A. Beilhack, H. Schulze, B. Nieswandt, and K. G. Heinze, “Thrombopoiesis is spatially regulated by the bone marrow vasculature,” *Nat. Commun.*, vol. 8, no. 1, 2017.

[86] W. S. Modi, K. Scott, J. J. Goedert, D. Vlahov, S. Buchbinder, R. Detels, S. Donfield, S. J. O’Brien, and C. Winkler, “Haplotype analysis of the SDF-1 (CXCL12) gene in a longitudinal HIV-1/AIDS cohort study,” *Genes Immun.*, vol. 6, no. 8, pp. 691–698, 2005.

[87] X. Blanchet, M. Langer, C. Weber, R. Koenen, and P. von Hundelshausen, “Touch of chemokines,” *Front. Immunol.*, vol. 3, no. JUL, 2012.

[88] L. Rajagopalan and K. Rajarathnam, “Structural Basis of Chemokine Receptor Function—A Model for Binding Affinity and Ligand Selectivity,” *Biosci. Rep.*, vol. 26, no. 5, pp. 325–339, 2006.

[89] M. Shirozu, T. Nakano, J. Inazawa, K. Tashiro, H. Tada, T. Shinohara, and T. Honjo, “Structure and chromosomal localization of the human stromal cell-derived factor 1 (SDF1) gene.,” *Genomics*, vol. 28, no. 3, pp. 495–500, 1995.

[90] L. Yu, J. Cecil, S.-B. Peng, J. Schrementi, S. Kovacevic, D. Paul, E. W. Su, and J. Wang, "Identification and expression of novel isoforms of human stromal cell-derived factor 1," *Gene*, vol. 374, pp. 174–179, 2006.

[91] Y.-R. Zou, A. H. Kottmann, M. Kuroda, I. Taniuchi, and D. R. Littman, "Function of the chemokine receptor CXCR4 in haematopoiesis and in cerebellar development," *Nature*, vol. 393, no. 6685, pp. 595–599, 1998.

[92] B. A. Teicher and S. P. Fricker, "CXCL12 (SDF-1)/CXCR4 pathway in cancer," *Clinical Cancer Research*, vol. 16, no. 11. pp. 2927–2931, 2010.

[93] F. Bachelerie, A. Ben-Baruch, A. M. Burkhardt, C. Combadiere, J. M. Farber, G. J. Graham, R. Horuk, A. H. Sparre-Ulrich, M. Locati, A. D. Luster, A. Mantovani, K. Matsushima, P. M. Murphy, R. Nibbs, H. Nomiyama, C. a Power, A. E. I. Proudfoot, M. M. Rosenkilde, A. Rot, S. Sozzani, M. Thelen, O. Yoshie, and A. Zlotnik, "International Union of Basic and Clinical Pharmacology. [corrected]. LXXXIX. Update on the extended family of chemokine receptors and introducing a new nomenclature for atypical chemokine receptors.," *Pharmacol. Rev.*, vol. 66, no. 1, pp. 1–79, 2014.

[94] A. Zlotnik, O. Yoshie, and H. Nomiyama, "The chemokine and chemokine receptor superfamilies and their molecular evolution," *Genome Biology*, vol. 7, no. 12. 2006.

[95] M. Kucia, K. Jankowski, R. Reca, M. Wysoczynski, L. Bandura, D. J. Allendorf, J. Zhang, J. Ratajczak, and M. Z. Ratajczak, "CXCR4-SDF-1 signalling, locomotion, chemotaxis and adhesion," *Journal of Molecular Histology*, vol. 35, no. 3. pp. 233–245, 2004.

[96] J. M. Busillo and J. L. Benovic, "Regulation of CXCR4 signaling," *Biochimica et Biophysica Acta - Biomembranes*, vol. 1768, no. 4. pp. 952–963, 2007.

[97] M. V Volin, L. Joseph, M. S. Shockley, and P. F. Davies, "Chemokine receptor CXCR4 expression in endothelium.," *Biochem. Biophys. Res. Commun.*, vol. 242, no. 1, pp. 46–53, 1998.

[98] B. Debnath, S. Xu, F. Grande, A. Garofalo, and N. Neamati, "Small molecule inhibitors of CXCR4," *Theranostics*, vol. 3, no. 1. pp. 47–75, 2013.

[99] U. M. Domanska, R. C. Kruizinga, W. B. Nagengast, H. Timmer-Bosscha, G. Huls, E. G. E. De Vries, and A. M. E. Walenkamp, "A review on CXCR4/CXCL12 axis in oncology: No place to hide," *Eur. J. Cancer*, vol. 49,

no. 1, pp. 219–230, 2013.

[100] T. Ara, K. Tokoyoda, T. Sugiyama, T. Egawa, K. Kawabata, and T. Nagasawa, "Long-term hematopoietic stem cells require stromal cell-derived factor-1 for colonizing bone marrow during ontogeny," *Immunity*, vol. 19, no. 2, pp. 257–267, 2003.

[101] T. Nagasawa, S. Hirota, K. Tachibana, N. Takakura, S. I. Nishikawa, Y. Kitamura, N. Yoshida, H. Kikutani, and T. Kishimoto, "Defects of B-cell lymphopoiesis and bone-marrow myelopoiesis in mice lacking the CXC chemokine PBSF/SDF-1," *Nature*, vol. 382, no. 6592, pp. 635–638, 1996.

[102] T. Nagasawa, "Microenvironmental niches in the bone marrow required for B-cell development," *Nature Reviews Immunology*, vol. 6, no. 2. pp. 107–116, 2006.

[103] K. Tachibana, S. Hirota, H. Iizasa, H. Yoshida, K. Kawabata, Y. Kataoka, Y. Kitamura, K. Matsushima, N. Yoshida, S. I. Nishikawa, T. Kishimoto, and T. Nagasawa, "The chemokine receptor CXCR4 is essential for vascularization of the gastrointestinal tract," *Nature*, vol. 393, no. 6685, pp. 591–594, 1998.

[104] K. Balabanian, B. Lagane, S. Infantino, K. Y. C. Chow, J. Harriague, B. Moepps, F. Arenzana-Seisdedos, M. Thelen, and F. Bachelerie, "The chemokine SDF-1/CXCL12 binds to and signals through the orphan receptor RDC1 in T lymphocytes," *J. Biol. Chem.*, vol. 280, no. 42, pp. 35760–35766, 2005.

[105] J. M. Burns, B. C. Summers, Y. Wang, A. Melikian, R. Berahovich, Z. Miao, M. E. T. Penfold, M. J. Sunshine, D. R. Littman, C. J. Kuo, K. Wei, B. E. McMaster, K. Wright, M. C. Howard, and T. J. Schall, "A novel chemokine receptor for SDF-1 and I-TAC involved in cell survival, cell adhesion, and tumor development," *J. Exp. Med.*, vol. 203, no. 9, pp. 2201–2213, 2006.

[106] Y. Döring, L. Pawig, C. Weber, and H. Noels, "The CXCL12/CXCR4 chemokine ligand/receptor axis in cardiovascular disease," *Front. Physiol.*, vol. 5 JUN, 2014.

[107] F. Sierro, C. Biben, L. Martinez-Munoz, M. Mellado, R. M. Ransohoff, M. Li, B. Woehl, H. Leung, J. Groom, M. Batten, R. P. Harvey, C. Martinez-A, C. R. Mackay, and F. Mackay, "Disrupted cardiac development but normal hematopoiesis in mice deficient in the second CXCL12/SDF-1 receptor,

CXCR7," *Proc. Natl. Acad. Sci.*, vol. 104, no. 37, pp. 14759–14764, 2007.

[108] S. Yu, D. Crawford, T. Tsuchihashi, T. W. Behrens, and D. Srivastava, "The chemokine receptor CXCR7 functions to regulate cardiac valve remodeling," *Dev. Dyn.*, vol. 240, no. 2, pp. 384–393, 2011.

[109] D. A. Sipkins, X. Wei, J. W. Wu, J. M. Runnels, D. Côté, T. K. Means, A. D. Luster, D. T. Scadden, and C. P. Lin, "In vivo imaging of specialized bone marrow endothelial microdomains for tumour engraftment," *Nature*, vol. 435, no. 7044, pp. 969–973, 2005.

[110] T. Sugiyama, H. Kohara, M. Noda, and T. Nagasawa, "Maintenance of the Hematopoietic Stem Cell Pool by CXCL12-CXCR4 Chemokine Signaling in Bone Marrow Stromal Cell Niches," *Immunity*, vol. 25, no. 6, pp. 977–988, 2006.

[111] S. Méndez-Ferrer, T. V. Michurina, F. Ferraro, A. R. Mazloom, B. D. MacArthur, S. A. Lira, D. T. Scadden, A. Mag'Ayan, G. N. Enikolopov, and P. S. Frenette, "Mesenchymal and haematopoietic stem cells form a unique bone marrow niche," *Nature*, vol. 466, no. 7308, pp. 829–834, 2010.

[112] L. Ding and S. J. Morrison, "Haematopoietic stem cells and early lymphoid progenitors occupy distinct bone marrow niches," *Nature*, vol. 495, no. 7440, pp. 231–235, 2013.

[113] A. Greenbaum, Y. M. S. Hsu, R. B. Day, L. G. Schuettpelz, M. J. Christopher, J. N. Borgerding, T. Nagasawa, and D. C. Link, "CXCL12 in early mesenchymal progenitors is required for haematopoietic stem-cell maintenance," *Nature*, vol. 495, no. 7440, pp. 227–230, 2013.

[114] G. M. Crane, E. Jeffery, and S. J. Morrison, "Adult haematopoietic stem cell niches," *Nature Reviews Immunology*, vol. 17, no. 9. pp. 573–590, 2017.

[115] K. Tokoyoda, T. Egawa, T. Sugiyama, B. Il Choi, and T. Nagasawa, "Cellular niches controlling B lymphocyte behavior within bone marrow during development," *Immunity*, vol. 20, no. 6, pp. 707–718, 2004.

[116] T. Hamada, R. Mohle, J. Hesselgesser, J. Hoxie, R. L. Nachman, M. A. S. Moore, and S. Rafii, "Transendothelial Migration of Megakaryocytes in Response to Stromal Cell-derived Factor 1 (SDF-1) Enhances Platelet Formation," *J. Exp. Med.*, vol. 188, no. 3, pp. 539–548, 1998.

[117] W. J. Lane, S. Dias, K. Hattori, B. Heissig, M. Choy, S. Y. Rabbany, J. Wood, M.

A. Moore, and S. Rafii, “Stromal-derived factor 1-induced megakaryocyte migration and platelet production is dependent on matrix metalloproteinases,” *Blood*, vol. 96, no. 13, pp. 4152–4159, 2000.

[118] L. M. Niswander, K. H. Fegan, P. D. Kingsley, K. E. McGrath, and J. Palis, “SDF-1 dynamically mediates megakaryocyte niche occupancy and thrombopoiesis at steady state and following radiation injury,” *Blood*, vol. 124, no. 2, pp. 277–286, 2014.

[119] K. Hodohara, N. Fujii, N. Yamamoto, and K. Kaushansky, “Stromal cell-derived factor-1 (SDF-1) acts together with thrombopoietin to enhance the development of megakaryocytic progenitor cells (CFU-MK),” *Blood*, vol. 95, no. 3, pp. 769–775, 2000.

[120] J. E. Sadler, “Biochemistry and genetics of von Willebrand factor.,” *Annu. Rev. Biochem.*, vol. 67, no. 1, pp. 395–424, 1998.

[121] Z. M. Ruggeri, “Von Willebrand factor, platelets and endothelial cell interactions,” pp. 1335–1342, 2003.

[122] M. A. Kowalska, L. Rauova, and M. Poncz, “Role of the platelet chemokine platelet factor 4 (PF4) in hemostasis and thrombosis,” *Thrombosis Research*, vol. 125, no. 4. pp. 292–296, 2010.

[123] R. Eisman, S. Surrey, B. Ramachandran, E. Schwartz, and M. Poncz, “Structural and functional comparison of the genes for human platelet factor 4 and PF4alt.,” *Blood*, vol. 76, no. 2, pp. 336–44, 1990.

[124] L. Lasagni, M. Francalanci, F. Annunziato, E. Lazzeri, S. Giannini, L. Cosmi, C. Sagrinati, B. Mazzinghi, C. Orlando, E. Maggi, F. Marra, S. Romagnani, M. Serio, and P. Romagnani, “An Alternatively Spliced Variant of CXCR3 Mediates the Inhibition of Endothelial Cell Growth Induced by IP-10, Mig, and I-TAC, and Acts as Functional Receptor for Platelet Factor 4,” *J. Exp. Med.*, vol. 197, no. 11, pp. 1537–1549, 2003.

[125] T. E. Warkentin, “Drug-Induced Immune-Mediated Thrombocytopenia — From Purpura to Thrombosis,” *N. Engl. J. Med.*, vol. 356, no. 9, pp. 891–893, 2007.

[126] B. Sauer, “Functional expression of the cre-lox site-specific recombination system in the yeast Saccharomyces cerevisiae.,” *Mol. Cell. Biol.*, vol. 7, no. 6, pp. 2087–2096, 1987.

[127] B. Sauer and N. Henderson, “Site-specific DNA recombination in mammalian cells by the Cre recombinase of bacteriophage P1.,” *Proc. Natl. Acad. Sci.*, vol. 85, no. 14, pp. 5166–5170, 1988.

[128] H. Gu, Y. R. Zou, and K. Rajewsky, “Independent control of immunoglobulin switch recombination at individual switch regions evidenced through Cre-loxP-mediated gene targeting,” *Cell*, vol. 73, no. 6, pp. 1155–1164, 1993.

[129] M. Ungerer, “Generation of Functional Culture-Derived Platelets From CD34+ Progenitor Cells to Study Transgenes in the Platelet Environment,” *Circ. Res.*, vol. 95, no. 5, pp. e36–e44, 2004.

[130] Y. Yin, L. Huang, X. Zhao, Y. Fang, S. Yu, J. Zhao, and B. Cui, “AMD3100 mobilizes endothelial progenitor cells in mice, but inhibits its biological functions by blocking an autocrine/paracrine regulatory loop of stromal cell derived factor-1 in vitro,” *J. Cardiovasc. Pharmacol.*, vol. 50, no. 1, pp. 61–67, 2007.

[131] A. Larochelle, A. Krouse, M. Metzger, D. Orlic, R. E. Donahue, S. Fricker, G. Bridger, C. E. Dunbar, and P. Hematti, “AMD3100 mobilizes hematopoietic stem cells with long-term repopulating capacity in nonhuman primates,” *Blood*, vol. 107, no. 9, pp. 3772–3778, 2006.

[132] I. Bruns, D. Lucas, S. Pinho, J. Ahmed, M. P. Lambert, Y. Kunisaki, C. Scheiermann, L. Schiff, M. Poncz, A. Bergman, and P. S. Frenette, “Megakaryocytes regulate hematopoietic stem cell quiescence through CXCL4 secretion,” *Nat. Med.*, vol. 20, no. 11, pp. 1315–1320, 2014.

[133] K. Kaushansky, “Thrombopoietin: The primary regulator of platelet production,” *Trends in Endocrinology and Metabolism*, vol. 8, no. 2. pp. 45–50, 1997.

[134] K. Kaushansky and J. G. Drachman, “The molecular and cellular biology of thrombopoietin: The primary regulator of platelet production,” *Oncogene*, vol. 21, no. 21 REV. ISS. 2, pp. 3359–3367, 2002.

[135] J. Lotem, Y. Shabo, and L. Sachs, “Regulation of megakaryocyte development by interleukin-6,” *Blood*, vol. 74, no. 5, pp. 1545–1551, 1989.

[136] T. Ishibashi, H. Kimura, T. Uchida, S. Kariyone, P. Friese, S. A. Burstein, and S. A. Bursteintt, “Human interleukin 6 is a direct promoter of maturation of

megakaryocytes in vitro.," *Proc. Natl. Acad. Sci. U. S. A.*, vol. 86, no. 15, pp. 5953–7, 1989.

[137] C. P. Stahl, D. Zucker-Franklin, B. L. Evatt, and E. F. Winton, "Effects of human interleukin-6 on megakaryocyte development and thrombocytopoiesis in primates.," *Blood*, vol. 78, no. 6, pp. 1467–1475, 1991.

[138] M. Xiao, Y. Wang, C. Tao, Z. Wang, J. Yang, Z. Chen, Z. Zou, M. Li, A. Liu, C. Jia, B. Huang, B. Yan, P. Lai, C. Ding, D. Cai, G. Xiao, Y. Jiang, and X. Bai, "Osteoblasts support megakaryopoiesis through production of interleukin-9," *Blood*, vol. 129, no. 24, pp. 3196–3209, 2017.

[139] K. Kaushansky, "Historical review: Megakaryopoiesis and thrombopoiesis," *Blood*, vol. 111, no. 3. pp. 981–986, 2008.

[140] J.-F. Wang, Z.-Y. Liu, and J. E. Groopman, "The α-Chemokine Receptor CXCR4 Is Expressed on the Megakaryocytic Lineage From Progenitor to Platelets and Modulates Migration and Adhesion," *Blood*, vol. 92, no. 3, pp. 756–764, 1998.

[141] S. Infantino, B. Moepps, and M. Thelen, "Expression and Regulation of the Orphan Receptor RDC1 and Its Putative Ligand in Human Dendritic and B Cells," *J. Immunol.*, vol. 176, no. 4, pp. 2197–2207, 2006.

[142] A. Uto-Konomi, B. McKibben, J. Wirtz, Y. Sato, A. Takano, T. Nanki, and S. Suzuki, "CXCR7 agonists inhibit the function of CXCL12 by down-regulation of CXCR4," *Biochem. Biophys. Res. Commun.*, vol. 431, no. 4, pp. 772–776, 2013.

[143] Y. Wang, G. Li, A. Stanco, J. E. Long, D. Crawford, G. B. Potter, S. J. Pleasure, T. Behrens, and J. L. R. Rubenstein, "CXCR4 and CXCR7 Have Distinct Functions in Regulating Interneuron Migration," *Neuron*, vol. 69, no. 1, pp. 61–76, 2011.

[144] F. M. Décaillot, M. A. Kazmi, Y. Lin, S. Ray-Saha, T. P. Sakmar, and P. Sachdev, "CXCR7/CXCR4 heterodimer constitutively recruits β-arrestin to enhance cell migration," *J. Biol. Chem.*, vol. 286, no. 37, pp. 32188–32197, 2011.

[145] C. W. Hendrix, A. C. Collier, M. M. Lederman, D. Schols, R. B. Pollard, S. Brown, J. B. Jackson, R. W. Coombs, M. J. Glesby, C. W. Flexner, G. J. Bridger,

K. Badel, R. T. MacFarland, G. W. Henson, and G. Calandra, “Safety, pharmacokinetics, and antiviral activity of AMD3100, a selective CXCR4 receptor inhibitor, in HIV-1 infection,” *J. Acquir. Immune Defic. Syndr.*, vol. 37, no. 2, pp. 1253–1262, 2004.

[146] I. Kalatskaya, Y. A. Berchiche, S. Gravel, B. J. Limberg, J. S. Rosenbaum, and N. Heveker, “AMD3100 Is a CXCR7 Ligand with Allosteric Agonist Properties,” *Mol. Pharmacol.*, vol. 75, no. 5, pp. 1240–1247, 2009.

[147] T. Goldmann, D. Drömann, J. Radtke, S. Marwitz, D. S. Lang, H. Schultz, and E. Vollmer, “CXCR7 transcription in human non-small cell lung cancer and tumor-free lung tissues; possible regulation upon chemotherapy,” *Virchows Archiv*, vol. 452, no. 3. pp. 347–348, 2008.

[148] J. Wang, Y. Shiozawa, J. Wang, Y. Wang, Y. Jung, K. J. Pienta, R. Mehra, R. Loberg, and R. S. Taichman, “The role of CXCR7/RDC1 as a chemokine receptor for CXCL12/SDF-1 in prostate cancer,” *J. Biol. Chem.*, vol. 283, no. 7, pp. 4283–4294, 2008.

[149] E. Schutyser, Y. Su, Y. Yu, M. Gouwy, S. Zaja-Milatovic, J. Van Damme, and A. Richmond, “Hypoxia enhances CXCR4 expression in human microvascular endothelial cells and human melanoma cells,” *Eur. Cytokine Netw.*, vol. 18, no. 2, pp. 59–70, 2007.

[150] Z. Miao, K. E. Luker, B. C. Summers, R. Berahovich, M. S. Bhojani, A. Rehemtulla, C. G. Kleer, J. J. Essner, A. Nasevicius, G. D. Luker, M. C. Howard, and T. J. Schall, “CXCR7 (RDC1) promotes breast and lung tumor growth in vivo and is expressed on tumor-associated vasculature.,” *Proc. Natl. Acad. Sci. U. S. A.*, vol. 104, no. 40, pp. 15735–40, 2007.

[151] D. Rath, M. Chatterjee, O. Borst, K. Müller, H. Langer, A. F. Mack, M. Schwab, S. Winter, M. Gawaz, and T. Geisler, “Platelet surface expression of stromal cell-derived factor-1 receptors CXCR4 and CXCR7 is associated with clinical outcomes in patients with coronary artery disease,” *J. Thromb. Haemost.*, vol. 13, no. 5, pp. 719–728, 2015.

[152] R. B. Maksym, M. Tarnowski, K. Grymula, J. Tarnowska, M. Wysoczynski, R. Liu, B. Czerny, J. Ratajczak, M. Kucia, and M. Z. Ratajczak, “The role of stromal-derived factor-1--CXCR7 axis in development and cancer.,” *Eur. J. Pharmacol.*, vol. 625, no. 1–3, pp. 31–40, 2009.

[153] D. H. McDermott, S. S. De Ravin, H. S. Jun, Q. Liu, D. A. Long Priel, P. Noel, C. M. Takemoto, T. Ojode, S. M. Paul, K. P. Dunsmore, D. Hilligoss, M. Marquesen, J. Ulrick, D. B. Kuhns, J. Y. Chou, H. L. Malech, and P. M. Murphy, "Severe congenital neutropenia resulting from G6PC3 deficiency with increased neutrophil CXCR4 expression and myelokathexis," *Blood*, vol. 116, no. 15, pp. 2793–2802, 2010.

[154] Q. Liu, Z. Li, J. L. Gao, W. Wan, S. Ganesan, D. H. Mcdermott, and P. M. Murphy, "CXCR4 antagonist AMD3100 redistributes leukocytes from primary immune organs to secondary immune organs, lung, and blood in mice," *Eur. J. Immunol.*, vol. 45, no. 6, pp. 1855–1867, 2015.

[155] C. W. Hendrix, C. Flexner, R. T. MacFarland, C. Giandomenico, E. J. Fuchs, E. Redpath, G. Bridger, and G. W. Henson, "Pharmacokinetics and safety of AMD-3100, a novel antagonist of the CXCR-4 chemokine receptor, in human volunteers.," *Antimicrob. Agents Chemother.*, vol. 44, no. 6, pp. 1667–73, 2000.

[156] F. NDA20067, "Center for Drug Evaluation and," pp. 0–29, 2011.

[157] T. Sugiyama and T. Nagasawa, "Bone marrow niches for hematopoietic stem cells and immune cells.," *Inflamm. Allergy Drug Targets*, vol. 11, no. 3, pp. 201–6, 2012.

[158] Dissertation Wenwen Fu, "Megakaryopoietic islands in the bone marrow balance platelet production and maintain megakaryocyte homeostasis", LMU, 2017.

6. Appendix

Abbreviations

min	minute
ml	milliliter
mm	millimeter
mM	millimolar
nm	nanometer
n	number
µg	microgram
µl	microliter
µm	micrometer
2P-IVM	Two-photon Intravital Microscopy
3D	3 dimension
BM	bone marrow
BSA	bovine serum albumin
CAR	cell CXCL12-abundent reticular cell
CLP	common lymphoid progenitor
CMP	common myeloid progenitor
CXCL12	C-X-C motif chemokine 12
CXCR4	CXC chemokine receptor 4
CXCR7	CXC chemokine receptor 7
DMEM	Dulbecco's Modified Eagle Medium
DMS	Demarcation membrane system
EDTA	Ethylenediaminetetraacetic acid
EdU	5-ethynyl-2'-deoxyuridine
EGFP	Enhanced green fluorescent protein
FACS	Fluorescence-activated cell sorting
FCS	fetal calf serum
FGF-4	Fibroblast growth factor-4
FITC	Fluorescein isothiocyanate
FL	Fetal liver
Fli1	Friend leukemia integration 1

GABPa	GA-binding protein alpha chain
G-CSF	Granulocyte-colony stimulating factor
GFP	green fluorescent protein
GMP	granulocytes/macrophage progenitor
GP	Glycoprotein
HSCs	Hematopoietic stem cells
ICAM-1	Intercellular adhesion molecule 1
IL	Interleukin
LMPP	lymphoid-primed multipotent progenitor
LSK	Lin- Sca-1+ c-Kit+
miR	microRNA
MAPK	mitogen-activated protein kinase
MEP	Megakaryocytic-erythrocytic progenitor
MFI	mean fluorescence intensity
MK	Megakaryocyte
MKp	Megakaryocyte progenitor
MPP	Multipotent progenitor
NGS	normal goat serum
NIR	near infrared
PBS	Phosphate buffer saline
PE	Phycoerythrin
PFA	Paraformaldehyde
PI	Propidium Iodide
RFP	Red Fluorescent Protein
rm	Recombinant mouse
RT	room temperature
RUNX	Runt-related transcription factor 1
SEM	standard error of the mean
S1p	Sphingosine 1-phosphate
SCF	Stem cell factor
SDF-1	Stromal cell-derived factor-1
SHG	Second Harmonic Generation

SLAM	Signaling lymphocyte activation molecule
SL-MKp	stem cell like megakaryocyte progenitor
TGF-β1	Transforming growth factor-β1
TPO	Thrombopoietin
vWF	von Willebrand Factor
WT	Wild type

Acknowledgement

It is my great honor to say thank you to my supervisor Prof. Dr. med Steffen Massberg for giving me this opportunity to join our wonderful project. I do really learned a lot during the past 2 years. Nowhere else will I learn so much within such a short period. My true gratitude is beyond the word's description for his patient instruction and warm encouragement.

I would like to convey my sincere gratitude to Dr.med Florian Gärtner, my direct supervisor. Owe to his excellent supervise, I can now thinking and working in a more logic way. It is him who changed me and taught me the real way to do scientific research. Except for the work, he did help me a lot on my life in Munich. His patience and encouragement help me to cross lots of difficulties through.

I feel deeply indebted to my colleagues and I don't know how to thank them enough for their help. Here I would like to say thank you to Michael Lorenz, Anna Titova, Elisabeth Raatz, Kieu Tien Cuong and Hellen Ishikawa, for all their help to my MD study. It is my fortune to work together with them. I would like to show my appreciation to all my Chinese friends in our lab. We fight together, we laugh together and we crack the hard nuts together. I am really glad to know them all.

I would like express my heartfelt thanks to IRTG 914 program for offering me professional trainings and awarding me the scholarship, and many thanks to Dr. Verena Kochan for her patient help on my offer application and on all the staff regarding the MD study here. At last, I would show my sincere gratitude to Ms. Holly Day, for all her help in my thesis correction.

Finally, I would like to express my deep gratitude to my family and friends, for their ardent expectation and endless support. It would be impossible for me to hang on without them.

Affidavit

Zheming Liu

Surname, first name

Street

Zip code, town

Country

I hereby declare, that the submitted thesis entitled

The effect of stromal cell-derived factor1（SDF1）on the migration of megakaryocyte progenitors: An in vitro analysis

is my own work. I have only used the sources indicated and have not made unauthorized use of services of a third party. Where the work of others has been quoted or reproduced, the source is always given.

I further declare that the submitted thesis or parts thereof have not been presented as part of an examination degree to any other university.

Munich, 21.03.2019 — Zheming Liu

Place, Date — Signature doctoral candidate

Confirmation of congruency between printed and electronic version of the doctoral thesis

Zheming Liu

Surname, first name

Street

Zip code, town

Country

I hereby declare, that the electronic version of the submitted thesis, entitled

The effect of stromal cell-derived factor1（SDF1）on the migration of megakaryocyte progenitors: An in vitro analysis

is congruent with the printed version both in content and format.

Munich, 21.03.2019 — Zheming Liu

Place, Date — Signature doctoral candidate